

The analysis of electric power price data and of the S&P 500 index using filtering and maximum likelihood in the calibration of a multiscale stochastic volatility model[†] *

Lorella Fatone

Dipartimento di Matematica e Informatica
Università di Camerino

Via Madonna delle Carceri 9, 62032 Camerino (MC), Italy

Ph. n.+39-0737-402558, FAX n.+39-0737-632525, E-mail:lorella.fatone@unicam.it

Francesca Mariani

CERI- Centro di Ricerca Previsione Prevenzione e Controllo dei Rischi Geologici
Università di Roma “La Sapienza”, Piazza Umberto Pilozzi 9, 00038 Valmontone (RM), Italy

Ph. n.+39-06-959938299, FAX n.+39-06-959938207, E-mail:fra_mariani@libero.it

Maria Cristina Recchioni

Dipartimento di Scienze Sociali “D. Serrani”
Università Politecnica delle Marche

Piazza Martelli 8, 60121 Ancona (AN), Italy

Ph. n.+39-071-2207066 , FAX n.+39-06-2207058, E-mail:m.c.recchioni@univpm.it

Francesco Zirilli

Dipartimento di Matematica “G. Castelnuovo”
Università di Roma “La Sapienza”

Piazzale Aldo Moro 2, 00185 Roma (RM), Italy

Ph. n.+39-06-49913282, FAX n.+39-06-44701007, E-mail:f.zirilli@caspur.it

[†]The numerical experience and data analysis reported in this paper have been obtained using the computing resources of CASPUR (Roma, Italy) under contract: “Multiscale stochastic volatility models in finance and insurance” granted to the Università di Roma “La Sapienza”. The support and sponsorship of CASPUR are gratefully acknowledged.

*The research reported in this paper is partially supported by MUR - Ministero Università e Ricerca (Roma, Italy), 40%, 2007, under grant: “The impact of population ageing on financial markets, intermediaries and financial stability”. The support and sponsorship of MUR are gratefully acknowledged.

Abstract

In this paper we use filtering and maximum likelihood methods to solve a calibration problem for a multiscale stochastic volatility model. The multiscale stochastic volatility model considered has been introduced in [10], [11] and describes the dynamics of the asset price using as auxiliary variables two stochastic variances varying on two different time scales. The aim of this paper is to estimate the parameters of this multiscale model (including the risk premium parameters when necessary) and its two initial stochastic variances from the knowledge, at discrete times, of the asset price and, eventually, of the prices of call and/or put European options on the asset. This problem is translated in a maximum likelihood problem with the likelihood function defined through the solution of a filtering problem. The estimated values of the parameters and of the two initial stochastic variances are characterized as being a constrained maximizer of a likelihood function. Furthermore we develop a tracking procedure that is able to track the asset price and the values of its two stochastic variances for time values where there are no data available. The solution of the calibration problem and the tracking procedure are used to do the analysis of data time series. Numerical examples of the solution of the calibration problem and of the performance of the tracking procedure using synthetic and real data are presented. The synthetic data time series is analyzed using data samples made of observations done with a given time frequency. We consider observation frequencies ranging from “high” to “low” frequencies and we study the performance of the calibration procedure as a function of the observation frequency. The real data studied are two time series of electric power price data taken from the U.S. electricity market and the 2005 data relative to the US *S&P* 500 index and to the prices of a call and a put European options on the S&P 500 index. In the study of real data we consider daily data. The results obtained from the analysis of the synthetic and of the real data are very satisfactory. Moreover in the real data case we use the estimated values of the parameters and of the initial stochastic variances obtained solving the calibration problem to produce through the tracking procedure mentioned above forecasts of the asset prices (electric power price and S&P 500 index), of the associated stochastic variances and of the option prices. The forecasts of the asset prices and of the option prices are compared with the prices actually observed. This comparison shows that the forecasts are of very high quality even when we consider “spiky” electric power price

data. The website: <http://www.econ.univpm.it/recchioni/finance/w9> contains some auxiliary material including some animations that helps the understanding of this paper. A more general reference to the work of the authors and of their coauthors in mathematical finance is the website: <http://www.econ.univpm.it/recchioni/finance>.

Keywords. Multiscale stochastic volatility models, filtering problem, calibration model, option pricing.

AMS (MOS) Subject Classification. 62F10, 35R30, 91B70.

M.S.C. classification. 34M50, 60H10, 91B28.

J.E.L. classification. C53, G12, C61.

1 Introduction

In this paper the problem of the calibration of a multiscale stochastic volatility model in mathematical finance is considered. The data used in the calibration problem are discrete time observations of the asset prices and, eventually, of the prices of European options on the asset. The calibration problem is formulated as a constrained optimization problem for a likelihood function. The likelihood function is constructed using the solution of a filtering problem. This formulation of the calibration problem has been suggested in [20] in the study of the Heston model and further developed in [3], [8], [9]. We solve the filtering problem and the maximum likelihood problem mentioned above. Moreover, thank to the solution of the filtering problem, we derive a tracking procedure able to forecast the asset and the option prices and the values of the stochastic variances of the model for time values where no observations are available.

The multiscale stochastic volatility model considered has been introduced in [10], [11] where formulae to price European put/call options in the multiscale model are derived and a calibration problem that uses as data European call and/or put option prices is formulated as a nonlinear least squares problem and it is solved. This multiscale stochastic volatility model generalizes the Heston model [16] and describes the dynamics of the asset price and of its two stochastic variances using a system of three Ito stochastic differential equations. The two stochastic variances vary on two different time scales, in this sense the model is multiscale. Under some hypotheses which

will be stated later the model proposed is “explicitly” solvable and “easy to use” in the sense that “explicit and easy to use” formulae for the transition probability density function of the state variables of the model and for the price of European vanilla call and put options on the asset can be derived (see [11]). In this paper using the formulae derived in [11] we state and we solve a filtering problem that generalizes the filtering problem for the Heston model studied in [20] and in [9]. The solution of this filtering problem is used to write a likelihood function and the calibration problem for the model is formulated as the problem of maximizing the likelihood function subject to some constraints, see [20], [8], [9], [3] where similar problems for simpler models are considered. The motivation to study multiscale stochastic volatility models comes from the fact that recently several statistical studies of market data have shown that in many circumstances the Black and Scholes model [2] and the one factor stochastic volatility models, such as the Heston model [16], are inadequate to capture the volatility smile contained in the option prices on the underlying asset and the volatility dynamics (see [12], [6], [4]). In these circumstances models using two factors, one fluctuating on a fast time scale and the other fluctuating on a longer time scale, to describe the asset volatility seem to be better equipped to capture the volatility structure implied by the option prices [1]. As a consequence of this empirical evidence a substantial effort has been devoted to formulate and to study multiscale stochastic volatility models expressed by Ito stochastic differential equations [13], [11], [1], [25]. A substitute to the use of these models is the use of jump models (see for example [23], [5]). This last type of models can be seen as an alternative or as a generalization of the one factor stochastic volatility models. The main disadvantage of using jump models in practical situations is the fact that their quantitative evaluation is a delicate matter (see for example [23], [5] and the references therein). We restrict our attention to the study of the multiscale stochastic volatility model presented in [11] and in the solution of the corresponding calibration problem we exploit the fact that the integral representation formulae derived in [11] for the transition probability density function of the state variables of the model and for the option prices are one dimensional integrals of explicitly known smooth functions easy to compute numerically. We apply the calibration and tracking procedures mentioned above to the processing of synthetic and real data. In the case of synthetic data we generate a “high frequency” data sample integrating numerically the stochastic differential equations that express the multiscale model. In particular a working day made of 6 hours is considered

and 24 equally spaced data points per day are generated numerically, that is data with a fifteen minutes observation frequency are generated. We consider a data sample covering a period of one year made of 365 days. The sampled trajectory is generated with a choice of the model parameters that makes likely the appearance of spikes in the data generated and the data sample generated (see Figure 1) contains spikes. We solve the calibration problem choosing from this set of synthetic data a rolling window of input data made of 24 (consecutive) observations taken with a given frequency. We show that when the calibration is made using data windows of high frequency data (observations taken every fifteen minutes), the calibration procedure employed, using data windows that do not contain spikes, is able to estimate parameter values that suggest the possibility of the future appearance of spikes. On the contrary we show that this is not the case when we consider low frequency data such as, for example, daily observations. In this last case we note that when the model calibration is made using as data data windows that do not contain spikes or is made using as data data windows containing spikes some of the parameter values estimated change abruptly. These facts suggest the validity of the calibration procedure adopted. The real data studied are relative to two time series of electric power prices taken from the U.S. electricity market and to the time series of the S&P 500 index and of the associated European vanilla option prices in the year 2005. When we study real data we consider daily prices and after solving the calibration problem we use the tracking procedure to forecast asset and (eventually) option prices. In particular we compare the electric power prices forecasted with the tracking procedure mentioned above with the prices actually observed. This comparison shows that the forecasted prices are of very high quality. The analysis of the time series of the electric power prices shows that even in the case of real data the model is able to handle the presence of spikes in the prices and to reflect them in the parameter values resulting from the solution of the calibration problem. Note that in the study of the electric power price data we do not use option prices as data in the calibration problem. In the study of the 2005 S&P 500 data (i.e.: S&P 500 index and European option prices) we use asset and option prices as data and we compare the forecasted values of the option prices obtained calibrating the multiscale model with the nonlinear least squares approach used in [11] with those obtained calibrating the model with the filtering and maximum likelihood approach developed in this paper. The comparison shows that the maximum likelihood approach using a much smaller number of data than that used by the least squares

approach gives very satisfactory results. In particular the results obtained for the option prices with the maximum likelihood approach are of substantially of the same quality than those presented in [11]. The quality of the forecasted option prices is established by comparison with the prices actually observed. Note that in the forecasting procedure of the option prices with the maximum likelihood method presented in Section 4 we do not assume the knowledge of the underlying asset price the day of the forecast. On the contrary in [11] the knowledge of the asset price the day of the forecast is assumed. Finally we use the tracking procedure mentioned above to forecast the *S&P500* index value and we compare the forecasts with the index values actually observed. This comparison shows the very high quality of the forecasts. A more complete study of the 2005 data of the S&P 500 index and of the corresponding option prices can be found in [10], [11] and in the website: <http://www.econ.univpm.it/recchioni/finance/w7>. The website: <http://www.econ.univpm.it/recchioni/finance/w9> contains some auxiliary material including some animations that helps the understanding of this paper. A more general reference to the work of the authors and of their coauthors in mathematical finance is the website: <http://www.econ.univpm.it/recchioni/finance>.

The remainder of the paper is organized as follows. In Section 2 we describe the multiscale stochastic volatility model considered and under some hypotheses we write an integral representation formula for its transition probability density function and for the price of European vanilla call and put options under the risk-neutral measure. In Section 3 we formulate and we solve the filtering and the calibration problems that are used to do the data analysis. Moreover we present the tracking procedure, that is we derive some formulae to forecast the asset price and the values of its two stochastic variances for time values where no observations are available. In Section 4 we apply the calibration and tracking procedures presented in Section 3 to the study of synthetic and real data.

2 The multiscale stochastic volatility model

For the convenience of the reader Section 2 summarizes some results contained in [11] that will be used in the following sections. Let \mathbb{R} and \mathbb{R}^+ be the sets of real and of positive real numbers respectively and t be a real variable that denotes time. Let S_t , $t \geq 0$, be a stochastic process describing

the asset (stock, commodity, index) price at time $t \geq 0$ and $x_t = \log(S_t/S_0)$, $t > 0$, be the corresponding log-return. We associate to the asset price two stochastic variances described by the stochastic processes $v_{1,t}$, $v_{2,t}$, $t > 0$, one fluctuating on a fast time scale and the other fluctuating on a long time scale. The dynamics of the stochastic process x_t , $v_{1,t}$, $v_{2,t}$, $t > 0$, is defined by the following system of stochastic differential equations:

$$dx_t = (\hat{\mu} + a_1 v_1 + a_2 v_2)dt + b_1 \sqrt{v_{1,t}} dW_t^{0,1} + b_2 \sqrt{v_{2,t}} dW_t^{0,2}, \quad t > 0, \quad (2.1)$$

$$dv_{1,t} = \chi_1(\theta_1 - v_{1,t})dt + \varepsilon_1 \sqrt{v_{1,t}} dW_t^1, \quad t > 0, \quad (2.2)$$

$$dv_{2,t} = \chi_2(\theta_2 - v_{2,t})dt + \varepsilon_2 \sqrt{v_{2,t}} dW_t^2, \quad t > 0, \quad (2.3)$$

where the quantities a_i , b_i , χ_i , ε_i , θ_i , $i = 1, 2$, are real constants satisfying the following conditions: $\chi_i \geq 0$, $\varepsilon_i \geq 0$, $\theta_i \geq 0$, $i = 1, 2$. These conditions are due to the financial meaning of the constants. We add to the previous conditions the following constraints: $\frac{2\chi_i \theta_i}{\varepsilon_i^2} > 1$, $i = 1, 2$, in order to guarantee that when $v_{i,t}$, $i = 1, 2$, are positive with probability one at time $t = 0$, $v_{i,t}$, $i = 1, 2$, solution of (2.2), or of (2.3), remain positive with probability one for $t > 0$. The fact that $v_{1,t}$, $v_{2,t}$, $t > 0$, are stochastic variances on different time scales is translated in the condition: $\chi_1 \ll \chi_2$. Finally $W_t^{0,1}$, $W_t^{0,2}$, W_t^1 , W_t^2 , $t > 0$, are standard Wiener processes such that $W_0^{0,1} = W_0^{0,2} = W_0^1 = W_0^2 = 0$, $dW_t^{0,1}$, $dW_t^{0,2}$, dW_t^1 , dW_t^2 , $t > 0$, are their stochastic differentials. We assume that:

$$\langle dW_t^1 dW_t^2 \rangle = 0, \quad t > 0, \quad (2.4)$$

$$\langle dW_t^{0,1} dW_t^1 \rangle = \rho_{0,1} dt, \quad t > 0, \quad (2.5)$$

$$\langle dW_t^{0,1} dW_t^2 \rangle = 0, \quad t > 0, \quad (2.6)$$

$$\langle dW_t^{0,2} dW_t^1 \rangle = 0, \quad t > 0, \quad (2.7)$$

$$\langle dW_t^{0,2} dW_t^2 \rangle = \rho_{0,2} dt, \quad t > 0, \quad (2.8)$$

$$\langle dW_t^{0,1} dW_t^{0,2} \rangle = 0, \quad t > 0, \quad (2.9)$$

where $\langle \cdot \rangle$ denotes the expected value of \cdot , and $\rho_{0,1}$, $\rho_{0,2} \in [-1, 1]$ are constants known as correlation coefficients. We remind that the autocorrelation coefficients of the stochastic differentials are equal to one (see [11] for further details).

The equations (2.1), (2.2), (2.3) are equipped with the initial condition:

$$x_0 = \tilde{x}_0, \quad (2.10)$$

$$v_{1,0} = \tilde{v}_{1,0}, \quad (2.11)$$

$$v_{2,0} = \tilde{v}_{2,0}, \quad (2.12)$$

where $\tilde{x}_0, \tilde{v}_{i,0}, i = 1, 2$, are random variables that we assume to be concentrated in a point with probability one. For simplicity we identify the random variables $\tilde{x}_0, \tilde{v}_{i,0}, i = 1, 2$, with the points where they are concentrated. Without loss of generality we choose $\tilde{x}_0 = 0$, and we assume $\tilde{v}_{i,0} \in \mathbb{R}^+, i = 1, 2$. Equations (2.1), (2.2), (2.3), the initial condition (2.10), (2.11), (2.12), the conditions on the correlation coefficients (2.4)-(2.9) and the conditions satisfied by the parameters appearing in the equations define the multiscale stochastic volatility model introduced in [11]. This model generalizes the Heston stochastic volatility model. In fact choosing $a_1 = -1/2, a_2 = 0, b_1 = 1, b_2 = 0$ the equations (2.1), (2.2) reduce to the Heston model and they become decoupled from equation (2.3). Remind that the stochastic variances and in particular the initial stochastic variances appearing in (2.11), (2.12) cannot be observed in real markets.

In order to formulate the filtering problem considered in Section 3 we need to compute the transition probability density function associated to the system of stochastic differential equations (2.1), (2.2), (2.3), that is the probability density function of having $x_t = x, v_{1,t} = v_1, v_{2,t} = v_2$ given the fact that $x_{t'} = x', v_{1,t'} = v'_1, v_{2,t'} = v'_2$, when $(x, v_1, v_2), (x', v'_1, v'_2) \in \mathbb{R} \times \mathbb{R}^+ \times \mathbb{R}^+$ and $t, t' \geq 0, t - t' > 0$, that we denote with $p_f(x, v_1, v_2, t, x', v'_1, v'_2, t'), (x, v_1, v_2), (x', v'_1, v'_2) \in \mathbb{R} \times \mathbb{R}^+ \times \mathbb{R}^+, t, t' \geq 0, t - t' > 0$. Moreover we need to compute the price of European vanilla call and put options on the asset whose price is given by $S_t = \tilde{S}_0 e^{x_t}, t > 0$, where $\tilde{S}_0 \in \mathbb{R}^+$ is the stock price at time $t = 0$. Remind that $x_t = \log(S_t/S_0), t > 0$, and that we have chosen $\tilde{x}_0 = 0$ with probability one so that we have $S_0 = \tilde{S}_0$ with probability one, that is S_0 is concentrated in the point \tilde{S}_0 with probability one. The function $p_f(x, v_1, v_2, t, x', v'_1, v'_2, t'), (x, v_1, v_2), (x', v'_1, v'_2) \in \mathbb{R} \times \mathbb{R}^+ \times \mathbb{R}^+, t, t' \geq 0, t - t' > 0$, as a function of the variables (x, v_1, v_2, t) is denoted with $\tilde{p}_f(x, v_1, v_2, t) = p_f(x, v_1, v_2, t, x', v'_1, v'_2, t'), (x, v_1, v_2) \in \mathbb{R} \times \mathbb{R}^+ \times \mathbb{R}^+, t > t' \geq 0$, and is the solution of the *Fokker Planck* equation:

$$\begin{aligned} \frac{\partial \tilde{p}_f}{\partial t}(x, v_1, v_2, t) &= L(\tilde{p}_f)(x, v_1, v_2, t), \\ (x, v_1, v_2) &\in \mathbb{R} \times \mathbb{R}^+ \times \mathbb{R}^+, t > t', \end{aligned} \quad (2.13)$$

with the boundary conditions:

$$\tilde{p}_f(x, v_1, v_2, t) \longrightarrow 0 \quad \text{as } x \rightarrow +\infty, \text{ or } x \rightarrow -\infty, \text{ and } t > t', \quad (2.14)$$

$$\tilde{p}_f(x, v_1, v_2, t) \longrightarrow 0 \quad \text{as } v_1 \rightarrow +\infty, \text{ and } t > t', \quad (2.15)$$

$$\tilde{p}_f(x, v_1, v_2, t) \longrightarrow 0 \quad \text{as } v_2 \rightarrow +\infty, \text{ and } t > t', \quad (2.16)$$

and with the initial condition:

$$\tilde{p}_f(x, v_1, v_2, t') = \delta(x - x')\delta(v_1 - v'_1)\delta(v_2 - v'_2), \quad (x, v_1, v_2) \in \mathbb{R} \times \mathbb{R}^+ \times \mathbb{R}^+, \quad (2.17)$$

where $\delta(\cdot)$ denotes the Dirac's delta and the operator $L(\cdot)$ is given by:

$$\begin{aligned} L(\cdot) = & \frac{1}{2} \left(\frac{\partial^2}{\partial x^2} ((b_1^2 v_1 + b_2^2 v_2) \cdot) + \frac{\partial^2}{\partial v_1^2} (\varepsilon_1^2 v_1 \cdot) + \frac{\partial^2}{\partial v_2^2} (\varepsilon_2^2 v_2 \cdot) \right. \\ & + 2 \frac{\partial^2}{\partial x \partial v_1} (\varepsilon_1 \rho_{0,1} v_1 b_1 \cdot) + 2 \frac{\partial^2}{\partial x \partial v_2} (\varepsilon_2 \rho_{0,2} v_2 b_2 \cdot) \\ & \left. - 2 \frac{\partial}{\partial x} ((\hat{\mu} + a_1 v_1 + a_2 v_2) \cdot) - 2 \frac{\partial}{\partial v_1} (\chi_1 (\theta_1 - v_1) \cdot) - 2 \frac{\partial}{\partial v_2} (\chi_2 (\theta_2 - v_2) \cdot) \right), \\ & (x, v_1, v_2) \in \mathbb{R} \times \mathbb{R}^+ \times \mathbb{R}^+. \end{aligned} \quad (2.18)$$

The *Fokker Planck* equation (2.13) is a parabolic partial differential equation degenerate on the boundary of its domain of definition, that is degenerate when $v_1 = 0$ or $v_2 = 0$ and $t > t' \geq 0$. The transition probability density function $p_f(x, v_1, v_2, t, x', v'_1, v'_2, t')$, $(x, v_1, v_2), (x', v'_1, v'_2) \in \mathbb{R} \times \mathbb{R}^+ \times \mathbb{R}^+$, $t, t' \geq 0$, $t - t' > 0$, is the fundamental solution of the *Fokker Planck* equation (2.13) with the boundary conditions (2.14), (2.15), (2.16).

As shown in [11] problem (2.13), (2.14), (2.15), (2.16), (2.17) can be solved using a technique described in [19] pag. 605-608 where it is applied to the *Fokker Planck* equation associated to the Heston model. In this way (see [11]) we obtain the following representation formula for p_f :

$$\begin{aligned} p_f(x, v_1, v_2, t, x', v'_1, v'_2, t') = & \frac{1}{2\pi} \int_{\mathbb{R}} dk e^{ik(x-x'-\mu\tau)} \prod_{i=1}^2 e^{-2\chi_i \theta_i ((\nu_i + \zeta_i)\tau + \log(s_{i,b}/(2\zeta_i)))/\varepsilon_i^2} . \\ & \left[e^{-2v'_i (\zeta_i^2 - \nu_i^2) s_{i,g}/(\varepsilon_i^2 s_{i,b}) - M_i(\tilde{v}_i + v_i)} M_i \left(\frac{v_i}{\tilde{v}_i} \right)^{(\chi_i \theta_i / \varepsilon_i^2) - 1/2} I_{2\chi_i \theta_i / \varepsilon_i^2 - 1} (2M_i(\tilde{v}_i v_i)^{1/2}) \right], \\ & (x, v_1, v_2), (x', v'_1, v'_2) \in \mathbb{R} \times \mathbb{R}^+ \times \mathbb{R}^+, t, t' \geq 0, t - t' > 0, \end{aligned} \quad (2.19)$$

where ι is the imaginary unit, $I_q(z)$ is the modified Bessel function of real order q , and the quantities $\nu_i, \zeta_i, s_{i,g}, s_{i,b}, \tilde{v}_i, M_i, i = 1, 2$, are given by:

$$\nu_i = -\frac{1}{2} (\chi_i + \iota k b_i \varepsilon_i \rho_{0,i}), \quad k \in \mathbb{R}, \quad i = 1, 2, \quad (2.20)$$

$$\zeta_i = \frac{1}{2} (4\nu_i^2 + \varepsilon_i^2(b_i^2 k^2 + 2\nu_i k a_i))^{1/2}, \quad k \in \mathbb{R}, \quad i = 1, 2, \quad (2.21)$$

$$s_{i,g} = 1 - e^{-2\zeta_i \tau}, \quad s_{i,b} = \zeta_i - \nu_i + (\zeta_i + \nu_i)e^{-2\zeta_i \tau}, \quad \tau > 0, \quad i = 1, 2, \quad (2.22)$$

$$\tilde{v}_i = \frac{4\nu_i' \zeta_i^2 e^{-2\zeta_i \tau}}{(s_{i,b})^2}, \quad M_i = \frac{2s_{i,b}}{\varepsilon_i^2 s_{i,g}}, \quad \tau > 0, \quad i = 1, 2. \quad (2.23)$$

Note that formula (2.19) gives the transition probability density function of the stochastic process solution of (2.1), (2.2), (2.3) under the assumptions (2.4)-(2.9) as a one dimensional integral of an explicitly known integrand. In this sense we say that under the assumptions (2.4)-(2.9) the multiscale stochastic volatility model (2.1), (2.2), (2.3) is explicitly solvable.

The formulae to price at time $t = 0$ European vanilla call and put options with strike price $K > 0$ and maturity time $T > 0$ are derived from (2.19) using the no arbitrage pricing theory. In fact we compute the option prices as expected values of discounted payoff functions with respect to an equivalent martingale measure known as risk-neutral measure (see for example [7], [23]). Let us denote with $\lambda_i \in \mathbb{R}$, $i = 1, 2$, the risk premium parameters of the risk neutral measure associated to (2.1), (2.2), (2.3). We note that the statistical measure of the model (2.1), (2.2), (2.3), whose density is given by (2.19), can be used to derive the corresponding risk neutral measure. In fact in order to obtain a formula for the density of the risk neutral measure associated to (2.1), (2.2), (2.3) it is sufficient to replace in (2.19) the parameters χ_i , θ_i , $i = 1, 2$, with the parameters $\tilde{\chi}_i = \chi_i + \lambda_i$, $\tilde{\theta}_i = \chi_i \theta_i / (\chi_i + \lambda_i)$, $i = 1, 2$, (see [11] for further details). Moreover when we consider the risk neutral measure we must impose the constraints $\tilde{\chi}_i \geq 0$, $\tilde{\theta}_i \geq 0$, $i = 1, 2$. Formula (2.19) with the parameters $\tilde{\chi}_i$ and $\tilde{\theta}_i$, instead than the parameters χ_i , θ_i , $i = 1, 2$, respectively is the required formula for the density of the risk neutral measure of the model (2.1), (2.2), (2.3). With some simple manipulations of the formulae discussed previously (see [11] for further details) under the risk neutral measure we obtain the following formula for the price C at time $t = 0$ of a European vanilla call option with maturity time $T > 0$, time to maturity $\tau = T - t > 0$ (remind that $t = 0$) and strike price K , when at time $t = 0$ the price of the underlying asset is given by \tilde{S}_0 and the values of the values of the stochastic variances are given by $\tilde{v}_{1,0}$, $\tilde{v}_{2,0}$:

$$C(\tau, K, \tilde{S}_0, \tilde{v}_{1,0}, \tilde{v}_{2,0}) = \frac{\tilde{S}_0}{2\pi} e^{-r\tau} e^{2\hat{\mu}\tau} \int_{-\infty}^{+\infty} dk \frac{e^{-ik(\log(\tilde{S}_0/K) + \hat{\mu}\tau) - \log(K/\tilde{S}_0)}}{-k^2 - 3ik + 2} \cdot \prod_{i=1}^2 \left(e^{-2\tilde{\chi}_i \tilde{\theta}_i ((\nu_i^c + \zeta_i^c)\tau + \log(s_{i,b}^c / (2\zeta_i^c))) / \varepsilon_i^2} e^{-2\tilde{v}_{i,0} ((\zeta_i^c)^2 - (\nu_i^c)^2) s_{i,g}^c / (\varepsilon_i^2 s_{i,b}^c)} \right),$$

$$\tau > 0, \tilde{S}_0, \tilde{v}_{1,0}, \tilde{v}_{2,0} > 0, \quad (2.24)$$

where r is the discount rate and the quantities ν_i^c , ζ_i^c , $s_{i,b}^c$, $s_{i,g}^c$, $i = 1, 2$, are given by:

$$\nu_i^c = -\frac{1}{2} (\tilde{\chi}_i + \imath k b_i \varepsilon_i \rho_{0,i} - 2b_i \rho_{0,i} \varepsilon_i), \quad k \in \mathbb{R}, \quad i = 1, 2, \quad (2.25)$$

$$\zeta_i^c = \frac{1}{2} (4(\nu_i^c)^2 + \varepsilon_i^2 (b_i^2 k^2 + 2\imath k a_i + 4\imath k b_i^2 - 4(a_i + b_i^2)))^{1/2}, \quad k \in \mathbb{R}, \quad i = 1, 2, \quad (2.26)$$

$$s_{i,g}^c = 1 - e^{-2\zeta_i^c \tau}, \quad s_{i,b}^c = \zeta_i^c - \nu_i^c + (\zeta_i^c + \nu_i^c) e^{-2\zeta_i^c \tau}, \quad \tau > 0, \quad i = 1, 2. \quad (2.27)$$

Analogously the formula for the price P at time $t = 0$ of a European vanilla put option with maturity time $T > 0$, time to maturity $\tau = T - t > 0$ (remind that $t = 0$) and strike price K , when at time $t = 0$ the price of the underlying asset is given by \tilde{S}_0 and the stochastic variances are given by $\tilde{v}_{1,0}$, $\tilde{v}_{2,0}$ is:

$$P(\tau, K, \tilde{S}_0, \tilde{v}_{1,0}, \tilde{v}_{2,0}) = \frac{K}{2\pi} e^{-r\tau} e^{-\hat{\mu}\tau} \int_{-\infty}^{+\infty} dk \frac{e^{-ik(\log(\tilde{S}_0/K) + \hat{\mu}\tau) - \log(\tilde{S}_0/K)}}{-k^2 + 3ik + 2} \cdot \prod_{i=1}^2 \left(e^{-2\tilde{\chi}_i \tilde{\theta}_i ((\nu_i^p + \zeta_i^p)\tau + \log(s_{i,b}^p / (2\zeta_i^p))) / \varepsilon_i^2} e^{-2\tilde{v}_{i,0} ((\zeta_i^p)^2 - (\nu_i^p)^2) s_{i,g}^p / (\varepsilon_i^2 s_{i,b}^p)} \right),$$

$$\tau > 0, \tilde{S}_0, \tilde{v}_{1,0}, \tilde{v}_{2,0} > 0, \quad (2.28)$$

where the quantities ν_i^p , ζ_i^p , $s_{i,g}^p$, $s_{i,b}^p$, are given by:

$$\nu_i^p = -\frac{1}{2} (\tilde{\chi}_i + \imath k b_i \varepsilon_i \rho_{0,i} + b_i \rho_{0,i} \varepsilon_i), \quad k \in \mathbb{R}, \quad i = 1, 2, \quad (2.29)$$

$$\zeta_i^p = \frac{1}{2} (4(\nu_i^p)^2 + \varepsilon_i^2 (b_i^2 k^2 + 2\imath k a_i - 2\imath k b_i^2 - 2(a_i + b_i^2)))^{1/2}, \quad k \in \mathbb{R}, \quad i = 1, 2, \quad (2.30)$$

$$s_{i,g}^p = 1 - e^{-2\zeta_i^p \tau}, \quad s_{i,b}^p = \zeta_i^p - \nu_i^p + (\zeta_i^p + \nu_i^p) e^{-2\zeta_i^p \tau}, \quad \tau > 0, \quad i = 1, 2. \quad (2.31)$$

Note that in the study of the calibration problem in (2.24), (2.28) we will choose $\hat{\mu} = r$.

3 The filtering and calibration problems

Let m be a positive integer and \mathbb{R}^m be the m -dimensional real Euclidean space. First of all in (2.1), (2.2), (2.3) we choose $a_i = -1/2$, $b_i = 1$, $i = 1, 2$, this choice translates in the multiscale model the usual relation between asset price, asset log-return and stochastic variance known from the Heston model. Remember that since in the calibration problem in the option price formulae (2.24), (2.28) we choose $\hat{\mu} = r$ we have that when the option prices are used as data of the calibration problem the discount rate r becomes a parameter that must be determined in the calibration. More general problems where r is not necessarily equal to $\hat{\mu}$ and a_i , b_i , $i = 1, 2$, are parameters to be determined in the calibration can be studied. We will not consider them here. We note that the model (2.1), (2.2), (2.3) together with the associated option price formulae (2.24), (2.28) are parameterized by 13 real quantities, that is: the model parameters $\hat{\mu}$, χ_i , θ_i , ε_i , $i = 1, 2$, the risk premium parameters λ_i , $i = 1, 2$, the correlation coefficients $\rho_{0,i}$, $i = 1, 2$, and the initial stochastic variances $\tilde{v}_{i,0}$, $i = 1, 2$. Remember that we have chosen $\hat{\mu} = r$. When we consider the filtering and calibration problems using as data asset and option prices we introduce the vector $\underline{\Theta} \in \mathbb{R}^{13}$ and the set $\mathcal{M} \subset \mathbb{R}^{13}$ defined as follows:

$$\mathcal{M} = \left\{ \underline{\Theta} = (\varepsilon_1, \theta_1, \rho_{0,1}, \chi_1, \tilde{v}_{0,1}, \hat{\mu}, \lambda_1, \varepsilon_2, \theta_2, \rho_{0,2}, \chi_2, \tilde{v}_{0,2}, \lambda_2) \in \mathbb{R}^{13} \mid \varepsilon_i, \chi_i, \theta_i \geq 0, \frac{2\chi_i\theta_i}{\varepsilon_i^2} \geq 1, -1 \leq \rho_{0,i} \leq 1, \tilde{v}_{i,0} \geq 0, \chi_i + \lambda_i > 0, i = 1, 2 \right\}. \quad (3.1)$$

The vector $\underline{\Theta} \in \mathbb{R}^{13}$ is the unknown of the calibration problem considered here and the set \mathcal{M} defines the set of “feasible” vectors, that is the set of vectors satisfying the constraints. Later in the formulation of the calibration problem we will assume $\underline{\Theta} \in \mathcal{M}$. When we consider the filtering and calibration problems using as data only asset prices the risk premium parameters λ_i , $i = 1, 2$, that appear in the option price formulae, must be removed from the vector $\underline{\Theta}$ and the definition of the vector $\underline{\Theta}$ and of the set \mathcal{M} must be changed consequently. To fix the ideas in this section we will discuss in detail the situation where asset prices and option prices are used as data in the filtering and in the calibration problem. We leave to the reader to work out the obvious changes that are needed when simpler problems are considered.

Let t_i , $i = 0, 1, \dots, n$, be time values such that $t_i < t_{i+1}$, $i = 0, 1, \dots, n -$

1, without loss of generality we choose $t_0 = 0$, and for later convenience we define $t_{n+1} = +\infty$. Let $(\tilde{x}_i, \tilde{C}_i, \tilde{P}_i)$ be respectively the log-return of the asset price S_t and the prices of European vanilla call and put options on the asset having maturity time T_i ($T_i > t_i$) and strike price K_i , observed at time $t = t_i$, $i = 0, 1, \dots, n$. We suppose that the option prices observations \tilde{C}_i, \tilde{P}_i , $i = 0, 1, \dots, n$, are affected by a Gaussian error with mean zero and known variance ϕ_i , $i = 0, 1, \dots, n$, respectively and that the asset log-returns \tilde{x}_i , $i = 0, 1, \dots, n$, are observed without error. The filtering problem that we consider is the following:

Given the vector $\underline{\Theta} \in \mathcal{M}$ find the probability density function $p(x, v_1, v_2, t | \mathcal{F}_t, \underline{\Theta})$, $(x, v_1, v_2) \in \mathbb{R} \times \mathbb{R}^+ \times \mathbb{R}^+$, $t > 0$, of the random variables $x_t, v_{1,t}$ and $v_{2,t}$, $t > 0$, solution of (2.1), (2.2), (2.3), (2.10), (2.11), (2.12), conditioned to the observations $\mathcal{F}_t = \{(\tilde{x}_i, \tilde{C}_i, \tilde{P}_i) : t_i \leq t, i > 0\}$, $t > 0$, and forecast the values of the state variables $x_t, v_{1,t}, v_{2,t}$ for $t > 0$ and in particular for $t \neq t_i$, $i = 0, 1, \dots, n$ and for $t > t_n$.

For $t = t_0 = 0$ we define $\mathcal{F}_{t_0} = \{\tilde{x}_0 = 0\}$. Note that in the filtering problem stated above we do not make use of the option prices \tilde{C}_0, \tilde{P}_0 observed at time $t = t_0$. That is in the filtering problem at time $t = t_0 = 0$, we use as datum only $x_0 = \tilde{x}_0 = 0$. The initial stochastic variances, appearing in (2.11), (2.12), in the filtering problem are assigned in the vector $\underline{\Theta}$ and can be considered as parameters. The call and put option prices \tilde{C}_0, \tilde{P}_0 at time $t = t_0 = 0$ will be used as data in the calibration problem. Many other filtering problems that use as data different combinations of asset prices and option prices can be studied with simple extensions of the formulae that follows. We will not consider them here.

Let us define the following functions:

$$\begin{aligned} p_i(x, v_1, v_2, t | \underline{\Theta}) &= p(x, v_1, v_2, t | \mathcal{F}_{t_i}, \underline{\Theta}), \\ (x, v_1, v_2) &\in \mathbb{R} \times \mathbb{R}^+ \times \mathbb{R}^+, t_i < t < t_{i+1}, \\ i &= 0, 1, \dots, n, \end{aligned} \tag{3.2}$$

to be the joint probability density functions of the random variables $x_t, v_{1,t}, v_{2,t}$, solution (2.1), (2.2), (2.3), (2.10), (2.11), (2.12), when $t_i < t < t_{i+1}$ conditioned to the observations \mathcal{F}_{t_i} made up to time $t = t_i$, $i = 0, 1, \dots, n$. Let us derive integral representation formulae for the functions $p_i(x, v_1, v_2, t | \underline{\Theta})$, $(x, v_1, v_2) \in \mathbb{R} \times \mathbb{R}^+ \times \mathbb{R}^+$, $t_i < t < t_{i+1}$, $i = 0, 1, \dots, n$. From (2.1), (2.2), (2.3), (2.10), (2.11), (2.12) it follows that the functions $p_i(x, v_1, v_2, t | \underline{\Theta})$,

$(x, v_1, v_2) \in \mathbb{R} \times \mathbb{R}^+ \times \mathbb{R}^+$, $t_i < t < t_{i+1}$, $i = 0, 1, \dots, n$, can be computed as solutions of a set of initial value problems for the Fokker Planck equation (2.13) (see [18] pag.164-165 and [20] equations (2.6), (2.7), (2.8)), that is as solutions of the following set of problems, for $i = 0, 1, \dots, n$:

$$\frac{\partial p_i}{\partial t} = L(p_i), \quad t_i < t < t_{i+1}, \quad (3.3)$$

where $L(\cdot)$ is given by (2.13) with the initial condition:

$$p_i(x, v_1, v_2, t_i | \underline{\Theta}) = f_i(x, v_1, v_2; \underline{\Theta}), \quad (x, v_1, v_2) \in \mathbb{R} \times \mathbb{R}^+ \times \mathbb{R}^+, \quad (3.4)$$

where

$$\begin{aligned} f_0(x, v_1, v_2; \underline{\Theta}) &= \delta(x - \tilde{x}_0) \delta(v_1 - \tilde{v}_{1,0}) \delta(v_2 - \tilde{v}_{2,0}), \\ (x, v_1, v_2) &\in \mathbb{R} \times \mathbb{R}^+ \times \mathbb{R}^+, \end{aligned} \quad (3.5)$$

and

$$\begin{aligned} f_i(x, v_1, v_2; \underline{\Theta}) &= \frac{\delta(x - \tilde{x}_i) p_{i-1}(x, v_1, v_2, t_i^- | \underline{\Theta}) \pi_1(x, v_1, v_2, t_i | \underline{\Theta})}{\int_0^{+\infty} \int_0^{+\infty} p_{i-1}(\tilde{x}_i, v'_1, v'_2, t_i^- | \underline{\Theta}) \pi_1(\tilde{x}_i, v'_1, v'_2, t_i | \underline{\Theta}) dv'_1 dv'_2}, \\ (x, v_1, v_2) &\in \mathbb{R} \times \mathbb{R}^+ \times \mathbb{R}^+, \quad i = 1, 2, \dots, n, \end{aligned} \quad (3.6)$$

where $p_{i-1}(x, v_1, v_2, t_i^- | \underline{\Theta}) = \lim_{t \rightarrow t_i^-} p_{i-1}(x, v_1, v_2, t | \underline{\Theta})$, $\lim_{t \rightarrow t_i^-}$ means left limit for t that goes to t_i , $i = 1, 2, \dots, n$, and

$$\begin{aligned} \pi_1(\tilde{x}_i, v_1, v_2, t_i | \underline{\Theta}) &= \\ \frac{1}{\sqrt{2\pi\phi_i}} \frac{1}{\sqrt{2\pi\phi_i}} &e^{\left(-\frac{1}{2\phi_i} [(\tilde{C}_i - C(\tilde{x}_i, v_1, v_2, t_i; K_i, T_i, \underline{\Theta}))^2 + (\tilde{P}_i - P(\tilde{x}_i, v_1, v_2, t_i; K_i, T_i, \underline{\Theta}))^2]\right)}, \\ (\tilde{x}_i, v_1, v_2) &\in \mathbb{R} \times \mathbb{R}^+ \times \mathbb{R}^+, \quad i = 0, 1, \dots, n. \end{aligned} \quad (3.7)$$

Note that when we consider filtering problems that do not use option prices as data in (3.6) we choose $\pi_1(x, v_1, v_2, t | \underline{\Theta}) = 1$, $(x, v_1, v_2) \in \mathbb{R} \times \mathbb{R}^+ \times \mathbb{R}^+$, $t = t_i$, $i = 1, 2, \dots, n$. The solutions of the initial value problems (3.3)-(3.4) can be represented as follows:

$$\begin{aligned} p_i(x, v_1, v_2, t | \underline{\Theta}) &= \\ \int_{-\infty}^{+\infty} dx' \int_0^{+\infty} dv'_1 \int_0^{+\infty} dv'_2 &p_f(x, v_1, v_2, t, x', v'_1, v'_2, t_i) f_i(x', v'_1, v'_2; \underline{\Theta}), \\ (x, v_1, v_2) &\in \mathbb{R} \times \mathbb{R}^+ \times \mathbb{R}^+, \quad t_i < t < t_{i+1}, \quad i = 1, 2, \dots, n. \end{aligned} \quad (3.8)$$

A detailed discussion of the filtering problem for the Heston model analogous to problem (3.3)-(3.7) and the development of an efficient numerical method to compute its solution can be found in [20]. The work presented in [20] can be extended to problem (3.3)-(3.7). We will not consider this extension here. We note that since the partial differential equation (3.3) is the *Fokker Planck* equation associated to the multiscale model (2.1), (2.2), (2.3), its fundamental solution p_f , given by (2.19), is the density of the statistical measure associated to (2.1), (2.2), (2.3), that is it is the risk neutral measure that has $\lambda_1 = \lambda_2 = 0$. Moreover it is easy to see that since f_0 is independent of λ_1, λ_2 the probability density function p_0 is independent of λ_1, λ_2 while the probability density functions $p_i, i = 1, 2, \dots, n$, depend on λ_1, λ_2 through the initial condition (3.4), that is through the functions $f_i, i = 1, 2, \dots, n$, defined in (3.6) that contain the option prices.

Using the functions $p_i(x, v_1, v_2, t|\underline{\Theta}), (x, v_1, v_2) \in \mathbb{R} \times \mathbb{R}^+ \times \mathbb{R}^+, t_i < t < t_{i+1}, i = 0, 1, \dots, n$, we can forecast the values of the state variables of the model $x_t, v_{1,t}, v_{2,t}, t > 0$, respectively as the expected values $\hat{x}_{t|\underline{\Theta}}, \hat{v}_{1,t|\underline{\Theta}}, \hat{v}_{2,t|\underline{\Theta}}, t > 0$, conditioned to the observations contained in $\mathcal{F}_t, t > 0$, of the random variables $x_t, v_{1,t}, v_{2,t}, t > 0$, that is:

$$\hat{x}_{t|\underline{\Theta}} = \mathbb{E}(x_t|\mathcal{F}_t, \underline{\Theta}) = \int_0^{+\infty} dv_1 \int_0^{+\infty} dv_2 \int_{-\infty}^{+\infty} dx x p_i(x, v_1, v_2, t|\mathcal{F}_t, \underline{\Theta}),$$

$$t_i < t < t_{i+1}, i = 0, 1, \dots, n, \quad (3.9)$$

$$\hat{v}_{j,t|\underline{\Theta}} = \mathbb{E}(v_{j,t}|\mathcal{F}_t, \underline{\Theta}) = \int_0^{+\infty} dv_1 \int_0^{+\infty} dv_2 \int_{-\infty}^{+\infty} dx v_j p_i(x, v_1, v_2, t|\mathcal{F}_t, \underline{\Theta}),$$

$$j = 1, 2, t_i < t < t_{i+1}, i = 0, 1, \dots, n, \quad (3.10)$$

where $E(\cdot|+)$ denotes the expected value of \cdot conditioned to $+$. The formulae (3.9), (3.10) can be used to track the random variables $x_t, v_{1,t}, v_{2,t}$, for $t > 0$, and in particular for $t \neq t_i, i = 0, 1, \dots, n$ and for $t > t_n$ and they constitute the tracking procedure announced in Section 1. The calibration problem consists in determining the value of the vector $\underline{\Theta} \in \mathcal{M}$ that makes most likely the observations $(\tilde{x}_i, \tilde{C}_i, \tilde{P}_i)$, made at time $t = t_i, i = 0, 1, \dots, n$. In the calibration problem we add to the data of the filtering problem the call and put option prices at time $t = t_0$, that is we add to the data of the filtering problem the observations \tilde{C}_0 and \tilde{P}_0 . Numerical experiments with the multiscale model and previous experience developed in the study of the Heston model [20], [9] suggest that the use in the calibration problem of \tilde{C}_0, \tilde{P}_0 as data improves greatly the quality of the estimates of the initial

stochastic variances resulting from the solution of the calibration problem. The improvement of the quality of the estimated initial stochastic variances determines an improvement in the estimates of all the remaining parameters contained in the vector $\underline{\Theta}$. As suggested in [20] given the observations we measure the (log-)likelihood of a vector $\underline{\Theta} \in \mathcal{M}$ through the following function:

$$F(\underline{\Theta}) = \sum_{i=0}^{n-1} \log \left[\int_0^{+\infty} \int_0^{+\infty} p_i(\tilde{x}_{i+1}, v_1, v_2, t_{i+1}^- | \underline{\Theta}) \pi_1(\tilde{x}_{i+1}, v_1, v_2, t_{i+1} | \underline{\Theta}) dv_1 dv_2 \right] \\ + \log \left[\int_0^{+\infty} \int_0^{+\infty} p_0(\tilde{x}_0, v_1, v_2, t_0 | \underline{\Theta}) \pi_1(\tilde{x}_0, v_1, v_2, t_0 | \underline{\Theta}) dv_1 dv_2 \right], \underline{\Theta} \in \mathcal{M}. \quad (3.11)$$

We have $t_0 = 0$ so that from (2.10), (2.12), (2.11) we have $p(x, v_1, v_2, t_0 | \mathcal{F}_{t_0}, \underline{\Theta}) = \delta(x - \tilde{x}_0) \delta(v_1 - \tilde{v}_{1,0}) \delta(v_2 - \tilde{v}_{2,0})$, $(x, v_1, v_2) \in \mathbb{R} \times \mathbb{R}^+ \times \mathbb{R}^+$, this implies that the (log-)likelihood function (3.11) can be rewritten as follows:

$$F(\underline{\Theta}) = \log[\pi_1(\tilde{x}_0, \tilde{v}_{1,0}, \tilde{v}_{2,0}, t_0 | \underline{\Theta})] + \\ \sum_{i=0}^{n-1} \log \left[\int_0^{+\infty} \int_0^{+\infty} p_i(\tilde{x}_{i+1}, v_1, v_2, t_{i+1}^- | \underline{\Theta}) \pi_1(\tilde{x}_{i+1}, v_1, v_2, t_{i+1} | \underline{\Theta}) dv_1 dv_2 \right], \\ \underline{\Theta} \in \mathcal{M}. \quad (3.12)$$

Note that in [20] and in [9] in the case of the Heston model the functions corresponding to the functions p_i , $i = 0, 1, \dots, n$ appearing in (3.11), (3.12) have been defined using as data asset log-returns and only one type of options prices, that is European vanilla call option prices instead than using asset log-returns and European vanilla call and put prices as done here. That is in the formulation of the calibration problem given here we have added the put option prices to the data used in [20] and in [9] in order to improve the quality of the estimated vector $\underline{\Theta}$ resulting from the solution of the calibration problem. In fact in the problem considered here we have $\underline{\Theta} \in \mathbb{R}^{13}$, that is we have thirteen parameters to estimate, while in the problem for the Heston model considered in [20] and in [9] we have only six or seven (when we consider also the risk premium parameter) parameters to estimate so that it is natural to increase the number of data used in the formulation of the calibration problem when we go from the Heston model case studied in [20] and in [9] to the case considered here. Moreover, we note that for $i = 0, 1, \dots, n-1$ the weight $\pi_1(\tilde{x}_{i+1}, v_1, v_2, t_{i+1} | \underline{\Theta})$ appearing in (3.12) is introduced to assign

higher weights to the values of the v_1, v_2 variables that make likely the observation of the option prices $\tilde{C}_{i+1}, \tilde{P}_{i+1}$ at time t_{i+1} actually made. Remind that when the option prices are not used as data in the calibration problem in (3.12) we choose $\pi_1(\tilde{x}_{i+1}, v_1, v_2, t_{i+1} | \underline{\Theta}) = 1, (x, v_1, v_2) \in \mathbb{R} \times \mathbb{R}^+ \times \mathbb{R}^+$.

The calibration problem that we consider is the following one:

Given the observations $(\tilde{x}_i, \tilde{C}_i, \tilde{P}_i)$ at time $t = t_i, i = 0, 1, \dots, n$, determine the vector $\underline{\Theta}^ \in \mathcal{M} \subset \mathbb{R}^{13}$ solution of the following nonlinear constrained optimization problem:*

$$\max_{\underline{\Theta} \in \mathcal{M}} F(\underline{\Theta}). \quad (3.13)$$

Problem (3.13) is known as maximum (log-)likelihood problem since the vector $\underline{\Theta}^* \in \mathcal{M}$ solution of (3.13) is the vector that makes “more likely” the observations actually made. The vector $\underline{\Theta}^* \in \mathcal{M}$ is the solution of the calibration problem. Note that problem (3.13) is only one possible way of using the maximum likelihood method to formulate the calibration problem that we are considering. Many other formulations of the calibration problem are possible and legitimate.

4 Some numerical experiments using synthetic and real data

The technique used to solve the optimization problem (3.13) is a variable metric steepest ascent method (see [15], [21]). Starting from an initial guess $\tilde{\underline{\Theta}}^0 \in \mathcal{M}$ of the vector $\underline{\Theta}^* \in \mathcal{M}$, solution of (3.13), we update at every iteration the current approximation of the solution of (3.13) with a step in the direction of the gradient of the (log-)likelihood function (3.11) computed in a suitable metric that takes care of the presence of the constraints defined in \mathcal{M} . To be more specific let us fix a tolerance value, $\delta > 0$, and the maximum number of iterations of the optimization procedure allowed, $iter > 0$, the basic steps of the optimization algorithm used to solve problem (3.13) are:

- 1 set $k = 0$ and initialize $\underline{\Theta} = \tilde{\underline{\Theta}}^0$;
- 2 evaluate $F(\underline{\Theta}^k)$, if $k > 0$ and $|F(\underline{\Theta}^k) - F(\underline{\Theta}^{k-1})| < \delta |F(\underline{\Theta}^k)|$, where $|\cdot|$ denotes the absolute value of \cdot , go to item 7;

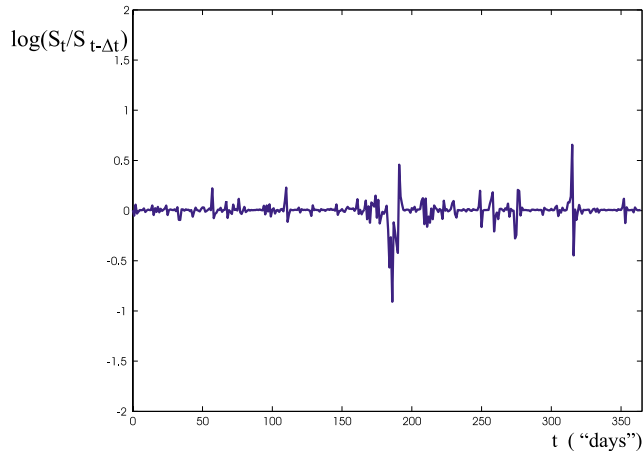


Figure 1: Log-return increment $\log(S_t/S_{t-\Delta t})$, $\Delta t = 1/24$ of the synthetic data versus time t (“days”).

- 3 evaluate the gradient (in cartesian coordinates) of the (log-)likelihood function $\nabla F(\underline{\Theta}^k)$;
- 4 perform the steepest ascent step evaluating $\underline{\Theta}^{k+1} = \underline{\Theta}^k + \eta_k D(\underline{\Theta}^k) \nabla F(\underline{\Theta}^k)$, where η_k is a positive real number that determines the length of the step in the direction $D(\underline{\Theta}^k) \nabla F(\underline{\Theta}^k)$ and guarantees that $F(\underline{\Theta}^k)$ is a non decreasing function of k and $D(\underline{\Theta}^k)$ is a diagonal matrix related to the use of the “variable metric”;
- 5 if $\|\underline{\Theta}^{k+1} - \underline{\Theta}^k\| < \delta$, go to item 7;
- 6 set $k = k + 1$, if $k < iter$ go to item 2;
- 7 approximate $\underline{\Theta}^*$ with $\underline{\Theta}^{k+1}$ and stop.

We build a “good” initial guess $\tilde{\underline{\Theta}}^0$ for the previous optimization algorithm doing a simple analysis of the input data, that is computing their mean value, their historical variance, and performing some “ad hoc” initial iterations starting from an initial guess $\underline{\Theta}^0 \in \mathcal{M}$ (see [9] for the details of a similar procedure used in the calibration of the Heston model). Moreover, once solved the calibration problem (3.13), that is after having determined an approximation of $\underline{\Theta}^*$, that with abuse of notation we denote with $\underline{\Theta}^*$, from the knowledge of the joint probability density function $p(x, v_1, v_2, t | \mathcal{F}_t, \underline{\Theta})$,

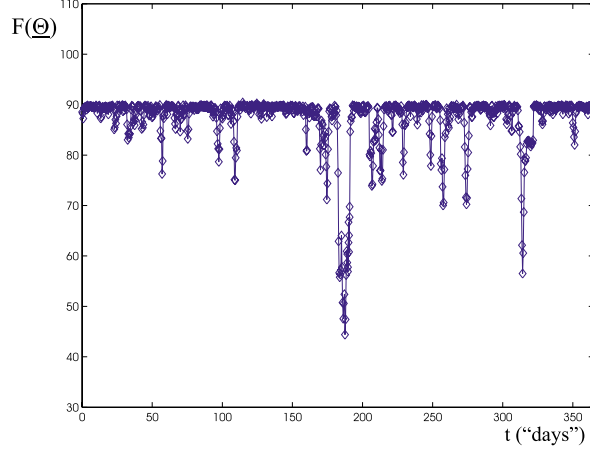


Figure 2: Value of the likelihood function $F(\underline{\Theta})$ at $\underline{\Theta} = \underline{\Theta}_i^*$, versus time $t = \tilde{t}_i$ (“days”), $i = 24, 25, \dots, 365 \cdot 24$ (results obtained using high frequency data).

$(x, v_1, v_2) \in \mathbb{R} \times \mathbb{R}^+ \times \mathbb{R}^+$, $t \geq 0$, we can forecast the values of the asset log-return x_t , $t > 0$, $t \neq t_i$, $i = 0, 1, \dots, n$, and of the stochastic variances $v_{1,t}$, $v_{2,t}$, $t > 0$, using respectively the expected values $\hat{x}_{t|\underline{\Theta}^*}$, $\hat{v}_{1,t|\underline{\Theta}^*}$, $\hat{v}_{2,t|\underline{\Theta}^*}$, $t > 0$, conditioned to the observations of the random variables x_{t_i} , v_{1,t_i} , v_{2,t_i} , $t_i > 0$, given in (3.9), (3.10). Some simple manipulations involving formulae (3.3), (3.4), (3.5), (3.6) and (2.19) show that we can rewrite (3.9), (3.10) as follows:

$$\begin{aligned}
\hat{x}_{t|\underline{\Theta}} &= \mathbb{E}(x_t | \mathcal{F}_{t_i}, \underline{\Theta}) = \tilde{x}_i + \left(\mu - \frac{\theta_1}{2} - \frac{\theta_2}{2}\right)(t - t_i) + \theta_1 \frac{(1 - e^{-\chi_1(t-t_i)})}{2\chi_1} \\
&\quad - \frac{(1 - e^{-\chi_1(t-t_i)})}{2\chi_1} \int_0^{+\infty} dv_2 \int_0^{+\infty} dv_1 v_1 f_i(v_1, v_2; \underline{\Theta}) \\
&\quad + \theta_2 \frac{(1 - e^{-\chi_2(t-t_i)})}{2\chi_2} - \frac{(1 - e^{-\chi_2(t-t_i)})}{2\chi_2} \int_0^{+\infty} dv_2 v_2 \int_0^{+\infty} dv_1 f_i(v_1, v_2; \underline{\Theta}), \\
&\quad t_i \leq t < t_{i+1}, \quad i = 0, 1, \dots, n, \tag{4.1}
\end{aligned}$$

$$\begin{aligned}
\hat{v}_{j,t|\underline{\Theta}} &= \mathbb{E}(v_{j,t} | \mathcal{F}_{t_i}, \underline{\Theta}) = \theta_j (1 - e^{-\chi_j(t-t_i)}) + \\
&\quad e^{-\chi_j(t-t_i)} \int_0^{+\infty} \int_0^{+\infty} dv_1 dv_2 v_j f_i(v_1, v_2; \underline{\Theta}), \quad j = 1, 2, \\
&\quad t_i \leq t < t_{i+1}, \quad i = 0, 1, \dots, n. \tag{4.2}
\end{aligned}$$

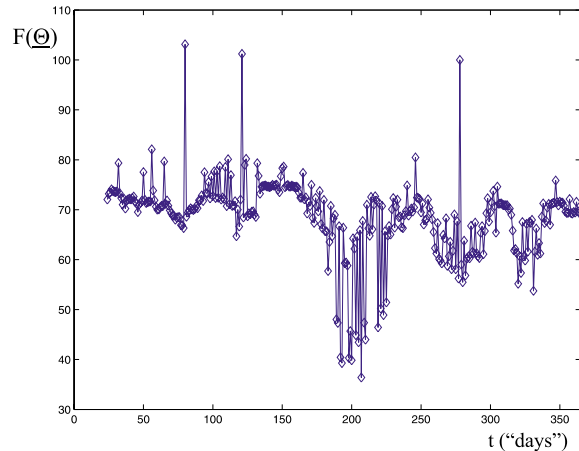


Figure 3: Value of the likelihood function $F(\underline{\Theta})$ at $\underline{\Theta} = \underline{\Theta}_i^{**}$ versus time $t = \hat{t}_i = i$ (“days”), $i = 24, 25, \dots, 365$ (results obtained using low frequency data).

That is, the forecasts $\hat{x}_{t,\underline{\Theta}^*}$, $\hat{v}_{1,t,\underline{\Theta}^*}$, $\hat{v}_{2,t,\underline{\Theta}^*}$ of x_t , $v_{1,t}$, $v_{2,t}$, $t > 0$, are obtained choosing $\underline{\Theta} = \underline{\Theta}^*$ in (4.1), (4.2) where $\underline{\Theta}^*$ is the approximation of the solution of problem (3.13) obtained with the optimization procedure described above. This is the tracking procedure announced previously and is the basic ingredient of the forecasts of the electric power prices and of the S&P 500 and of its European options prices presented in this Section.

We present three numerical experiments. The first one uses synthetic data and shows that the calibration procedure proposed is able to reconstruct satisfactorily the parameters of the multiscale model (2.1), (2.2), (2.3). We show some evidence of the fact that the calibration procedure is able to handle circumstances that imply the possibility of spikes or eventually the actual presence of spikes in the input data. In particular the behaviour of the solution of the calibration problem as a function of the time frequency of the input data is studied. In the second and third experiments we consider daily data. The second experiment consists in the analysis of two time series of electric power price data, the first time series does not contain spikes while the second one contains spikes. No option prices are used as data in this experiment. The electric power price data studied are taken from the U.S. electricity market. This experiment shows that the calibration of the model on data containing spikes gives parameter estimates

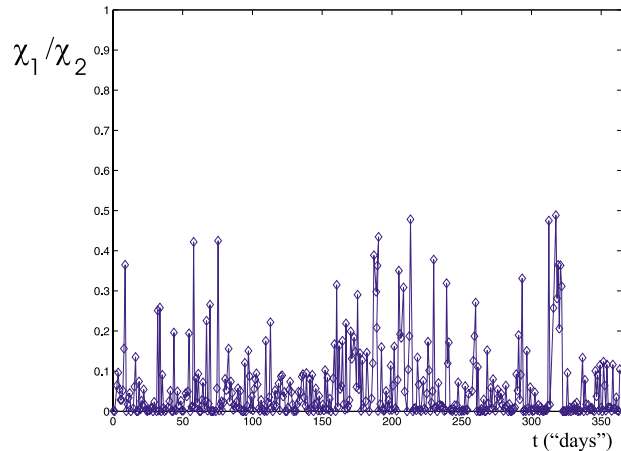


Figure 4: Value of the ratio χ_1/χ_2 of the vector $\underline{\Theta}_i^*$ versus time $t = \tilde{t}_i$ (“days”), $i = 24, 25, \dots, 365 * 24$ (results obtained using high frequency data).

substantially different from the estimates obtained applying the calibration procedure to data that do not contain spikes. In particular the estimates of the speeds of mean reversion χ_1, χ_2 and of the volatilities of volatilities ϵ_1, ϵ_2 take different values depending on the presence or absence of spikes in the data. Using the solution of the calibration problem and the tracking procedure introduced above we forecast electric power prices. We compare the electric power prices forecasted with the tracking procedure with the prices actually observed to establish the quality of the forecasted prices. This comparison shows that the forecasted prices are of very high quality. Finally, the third experiment shows how the calibration procedure works on the 2005 data relative to the S&P 500 index and to the price of European put and call options on this index. In this experiment using formulae (4.1), (4.2) we forecast the S&P 500 index and the option prices and the forecasted prices are compared to the historical data. This comparison establishes the high quality of the forecasted prices. Moreover we compare the maximum likelihood formulation of the calibration problem considered here with the least squares formulation of the calibration problem studied in [11]. The website <http://www.econ.univpm.it/recchioni/finance/w9> contains some auxiliary material including some animations that helps the understanding of the experiments presented.

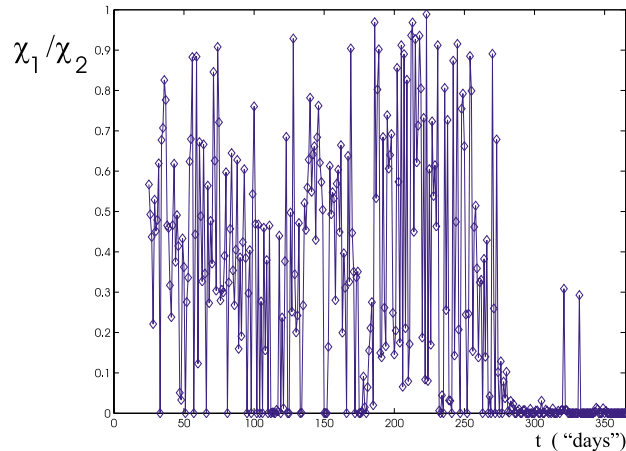


Figure 5: Value of the ratio χ_1/χ_2 of the vector $\underline{\Theta}_i^{**}$ versus time $t = \hat{t}_i = i$ (“days”), $i = 24, 25, \dots, 365$ (results obtained using low frequency data).

In the numerical experiments, without loss of generality, we impose $\chi_1 \leq \chi_2$. Let us present the first numerical experiment. The synthetic data used have been obtained integrating numerically one trajectory of the stochastic differential equations (2.1), (2.2), (2.3) with the initial condition (2.10), (2.11), (2.12) using the explicit Euler method with variable stepsize. We have generated a trajectory of the log-return x_t and of the stochastic variances $v_{1,t}$, $v_{2,t}$, this trajectory is sampled with 24 equally spaced points for each working day. A working day is made of six hours, sometime these days made of six hours are denoted with “days”. We have computed the trajectory for a “year” made of 365 working days. That is we have considered a sampling frequency of fifteen minutes. These data are regarded as high frequency data. In this experiment no option price data are used.

The vector $\underline{\Theta}$ of the model used to generate the synthetic data has the following components: $\epsilon_1 = 0.06$, $\theta_1 = 0.05912$, $\rho_{0,1} = 0.99955$, $\chi_1 = 0.3682$, $\tilde{v}_{0,1} = 0.20502$, $\hat{\mu} = 0.1924$, $\epsilon_2 = 1.28581$, $\theta_2 = 0.215164$, $\rho_{0,2} = -0.988$, $\chi_2 = 100.946$, $\tilde{v}_{0,2} = 0.286326$. Remind that we have chosen $\tilde{x}_0 = 0$.

Note that in this experiment the risk premium parameters λ_1 , λ_2 are not considered since the option prices are not used as data and this fact implies that $\underline{\Theta} \in \mathbb{R}^{11}$ instead than to \mathbb{R}^{13} . The choice of the vector $\underline{\Theta}$ made above defines a model that is truly multiscale, in fact we have $\chi_2/\chi_1 \approx 300$. This model is likely to generate spikes in the data. Figure 1 shows the quantity

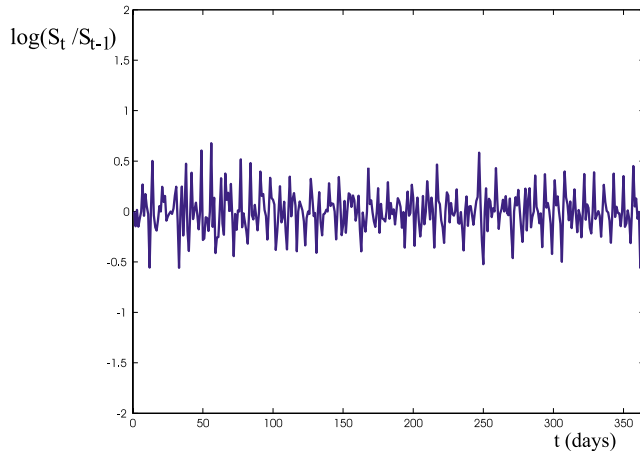


Figure 6: Log-return increment $\log(S_t/S_{t-1})$ of the electric power prices versus time t (days)(time series with no spikes, daily data).

$\log(S_{t_i}/S_{t_{i-1}})$, $t = t_i = \tilde{t}_i = i/24$, $i = 1, 2, \dots, 365 * 24$ associated with the synthetic data obtained from the computed trajectory of (2.1), (2.2), (2.3) with initial condition (2.10), (2.11), (2.12) when the time t is measured in “days”. It is easy to see that $x_t - x_{t-\Delta t} = \log(S_t/S_{t-\Delta t})$, so that the quantity plotted in Figure 1 is the log-return increment in one time step Δt . Note that in Figure 1 we have considered $\Delta t = 1/24$ day as time step and that since we consider a “day” made of six hours we have $\Delta t = 15$ minutes. The data shown in Figure 1 have spikes in $\log(S_t/S_{t-\Delta t})$ around the 183th, and the 320th day. We use as data of the calibration problems considered in this experiment some subsets of the time series of the log-returns associated with the data shown in Figure 1. Given the frequency of observation we have solved the calibration problems resulting from the use as input data of a rolling window of 24 “consecutive” observations of x_t (with the given frequency). Keep in mind that using the synthetic data shown in Figure 1 the highest frequency that can be considered is: one observation every fifteen minutes. We go from a set of input data (i.e.: a window) to the next one discarding the first observation of the input data and inserting as new observation the next observation (with the given frequency) that follows the last observation of the input data. Given the input data frequency we solve all the calibration problems corresponding to rolling with the previous procedure the data window through the data time series. We choose the

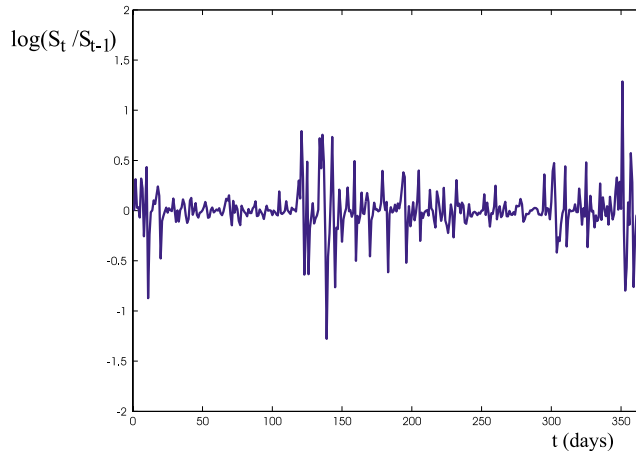


Figure 7: Log-return increment $\log(S_t/S_{t-1})$ of the electric power prices versus time t (days) (time series with spikes, first year of observation, daily data).

same initial guess $\tilde{\Theta}^0$ for the optimization method for all the calibration problems considered. When the frequency of observation is chosen to be one observation every fifteen minutes and the input data windows are made of 24 “consecutive” observations, the calibration procedure applied to the rolling window provides $364 \cdot 24 + 1$ estimates $\underline{\Theta}_i^*$, $i = 24, 25, \dots, 365 \cdot 24$ of the vector $\underline{\Theta}$. The index i associated to $\underline{\Theta}_i^*$ is the index of the last observation contained in the data window used in the calibration problem. For later convenience, the corresponding optimal values $F(\underline{\Theta}_i^*)$, $i = 24, 25, \dots, 365 \cdot 24$ of the (log-)likelihood function $F(\underline{\Theta})$ have been computed and are shown in Figure 2.

The same calibration exercise has been repeated using a rolling window made of 24 daily observations. Note that these daily observations are obtained sub-sampling appropriately the previous numerically computed trajectory that has one data point every fifteen minutes. Remind that we consider a “day” made of six hours. Thus this second calibration exercise provides 365 estimates $\underline{\Theta}_i^{**}$, $i = 24, 25, \dots, 365$ of the vector $\underline{\Theta}$ and the corresponding optimal values $F(\underline{\Theta}_i^{**})$, $i = 24, 25, \dots, 365$ of the (log-)likelihood function $F(\underline{\Theta})$ have been computed and are shown in Figure 3. Note that in this last case the index i denotes the date $t = \hat{t}_i = i$ (days) (i -th day of the data time series) of the last observation of the rolling window. The initial guess $\tilde{\Theta}^0$ of the optimization procedure is a point with $\chi_1 = \chi_2 = 10$ and we use always

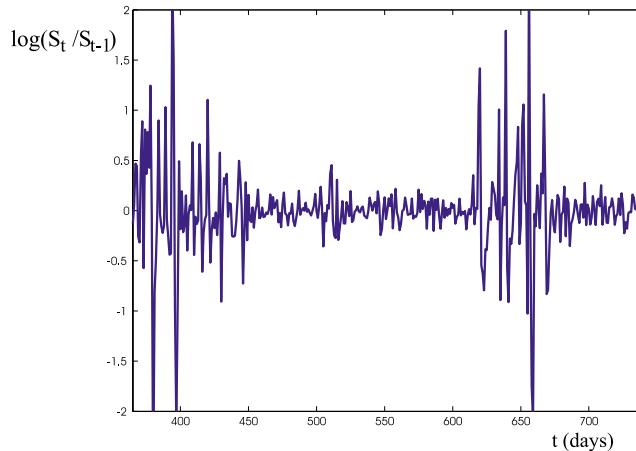


Figure 8: Log-return increment $\log(S_t/S_{t-1})$ of the electric power prices versus time t (days) (time series with spikes, second year of observation, daily data).

the same initial guess in all the calibration problems solved.

The numerical results obtained in this experiment are shown in Figures 2-5 and they point out the following facts. The first fact comes out from the observation of Figure 2 where the optimal values $F(\underline{\Theta}_i^*)$ as a function of time $t = \tilde{t}_i$, where $\tilde{t}_i = i/24$, $i = 24, 25, \dots, 365 * 24$ is the date (measured in days) of the last observation in the data window used in the calibration, are shown. In fact in Figure 2 the optimal value of the (log-)likelihood function changes abruptly when the time \tilde{t}_i approaches a time value where the data have a spike (see Figure 1). This happens since for these time values the (log-)likelihood function changes abruptly so that the choice, that we have made, of solving the optimization problems starting from the same initial guess is probably insufficient to handle these situations. Note the difference between Figure 2 (where we study high frequency data) that shows an approximately constant log-likelihood function at the solution of the calibration problems and Figure 3 (where low frequency data are studied) that shows a widely changing log-likelihood function at the solution of the calibration problems. Remember that since the data have been generated using only one choice of the vector $\underline{\Theta}$ and the data window considered are all the same type a completely satisfactory solution of the calibration problem should show $F(\underline{\Theta}_i^*)$ in Figure 2 and $F(\underline{\Theta}_i^{**})$ in Figure 3 approximately constants as a function of

i.

The second fact comes out from the behavior of the values of the speeds of the mean reverting processes, that is the values of the parameters χ_1 , χ_2 , obtained as solution of the calibration problems. Remind that we have chosen $\chi_1 \leq \chi_2$. When the high frequency data are used in the calibration procedure we observe that the mean and median values of the ratio χ_1/χ_2 reconstructed from the data in the calibration problems are equal to 0.0586 and to 0.0164 respectively, that is there is a mean difference of one order of magnitude between the two speeds χ_1 , χ_2 and there is a difference of two orders of magnitude if we consider the median value instead than the mean value (see Figure 4). We can conclude that when we use high frequency data the calibration reveals the presence of two scales in the model. This fact is a signal that spikes in the log-return are likely, and it is important to note that this is found even elaborating data that do not contain spikes. On the other hand when daily observations (low frequency data) are used in the calibration procedure (see Figure 5) we observe that the mean and median values resulting from the calibration of the ratio χ_1/χ_2 are equal to 0.2 and to 0.29 respectively, that is there is not a relevant difference in the mean or median in the magnitude of the two speeds of mean reversion. However looking at Figure 5 we can see that when spikes are contained in the observation window used to calibrate the model (i.e. when $i \geq 220$) the ratio χ_1/χ_2 is near zero. This means that from the elaboration of daily data the calibration procedure produces values of the speeds of mean reversion of different order of magnitude only when processing data containing spikes. Remind that in the vector Θ used to generate the data we have $\chi_1/\chi_2 = 0.003647$. These last findings suggest the importance of using high frequency data to recognize the multiscale character of the model and be prepared to the appearance of spikes in the data before their actual appearance.

The second numerical experiment considers two time series of electric power price data. The first time series consists of 365 daily observations \tilde{S}_i , $i = 0, 1, \dots, 364$, that is it is a year, made of 365 days, of daily observations. The second time series consists of 765 daily observations \hat{S}_i , $i = 0, 1, \dots, 764$. In this experiment no option price data are used. Figure 6 shows the daily log-return increment $\tilde{x}_i - \tilde{x}_{i-1} = \log(\tilde{S}_i/\tilde{S}_{i-1})$, $i = 1, 2, \dots, 364$, of the electric power price data \tilde{S}_i , $i = 0, 1, \dots, 364$. The time series shown in Figure 6 does not contain spikes. Figures 7 and 8 show the daily log-return increment of the second time series of electric power price data. Figure 7 shows the daily

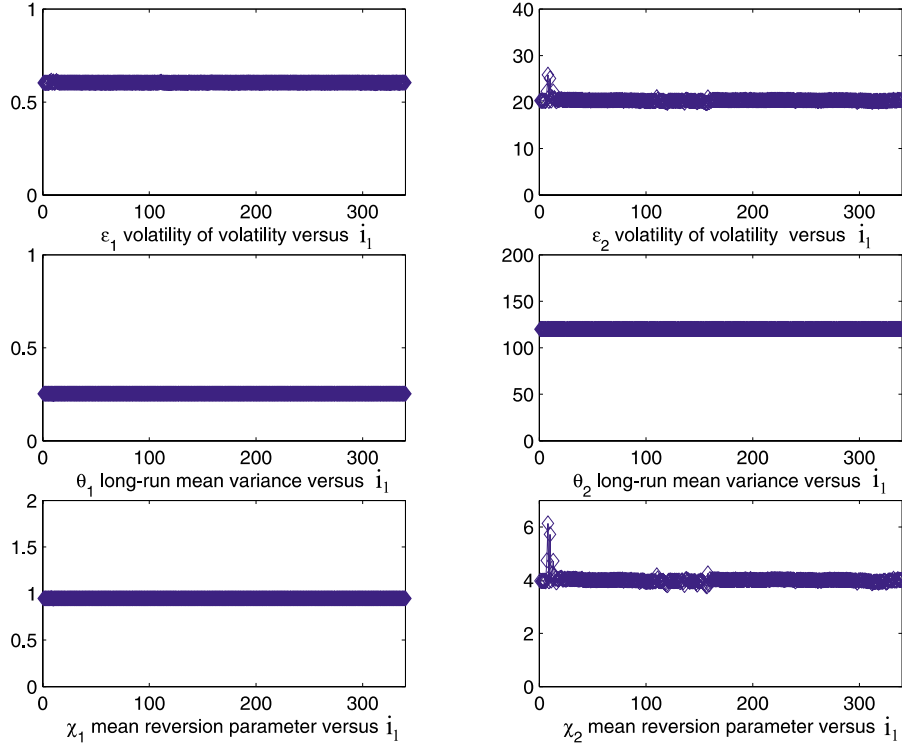


Figure 9: Estimated parameter values obtained solving 341 calibration problems using as data the electric power prices (time series with no spikes, Figure 6) versus the calibration problem number i_1 .

log-return increment of the second time series of electric power price data in the first year of observation and Figure 8 shows the daily log-return increment in the second year of observation. The time series shown in Figures 7 and 8 contains spikes. We begin the analysis of these time series calibrating the multiscale model using a data window made of 26 consecutive daily observations and we move this window along the time series substituting the first observation of the window with the next observation after the window. Using this procedure in the case of the time series shown in Figure 6 we solve 340 ($340=365-26+1$) calibration problems numbered with the index i_1 , $i_1 = 1, 2, \dots, 340$ and in the case of the time series shown in Figures 7 and 8 we solve 740 ($740=765-26+1$) calibration problems numbered with the index i_1 , $i_1 = 1, 2, \dots, 740$. The index i_1 is the number of the first day contained in the data window used in the calibration. Figures 9 and 10 show the results

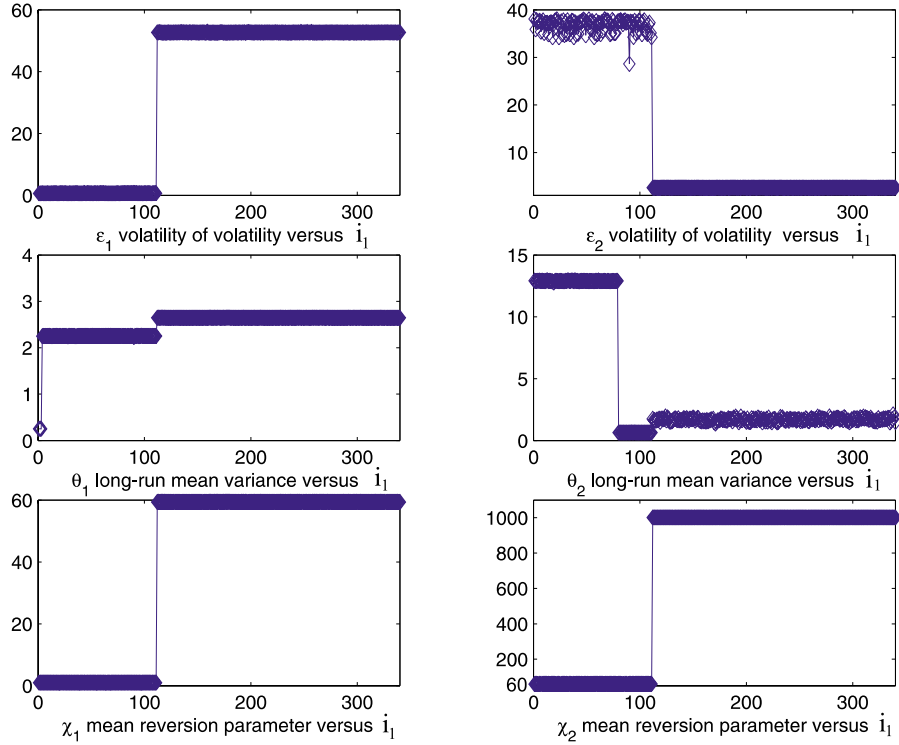


Figure 10: Estimated parameter values obtained solving 341 calibration problems using as data the electric power prices (time series with spikes, Figure 7) versus the calibration problem number i_1 .

obtained solving the calibration problems associated to the two time series of data as a function of the index i_1 for $i_1 = 1, 2, \dots, 340$. Figure 9 shows the results obtained processing the time series of electric power price data with no spikes (shown in Figure 6). Remind that this time series is made of one year of daily data. Figure 10 shows the results obtained processing the first year of the time series of electric power price data with spikes (shown in Figure 7). We focus our attention on Figures 9, 10 to point out the different behaviour of the estimated parameter values in the two cases. In absence of spikes (Figure 9) the parameters $\epsilon_i, \theta_i, \chi_i, i = 1, 2$, are stable, that is they are approximately constants as a function of i_1 , and χ_1 and χ_2 are of the same order of magnitude (i.e.: $\chi_1 \approx 1, \chi_2 \approx 4$). In presence of spikes (Figure 10) the parameters $\epsilon_i, \theta_i, \chi_i, i = 1, 2$, have a jump in correspondence of the first spike. However comparing Figure 7 and Figure 10 we can see that the

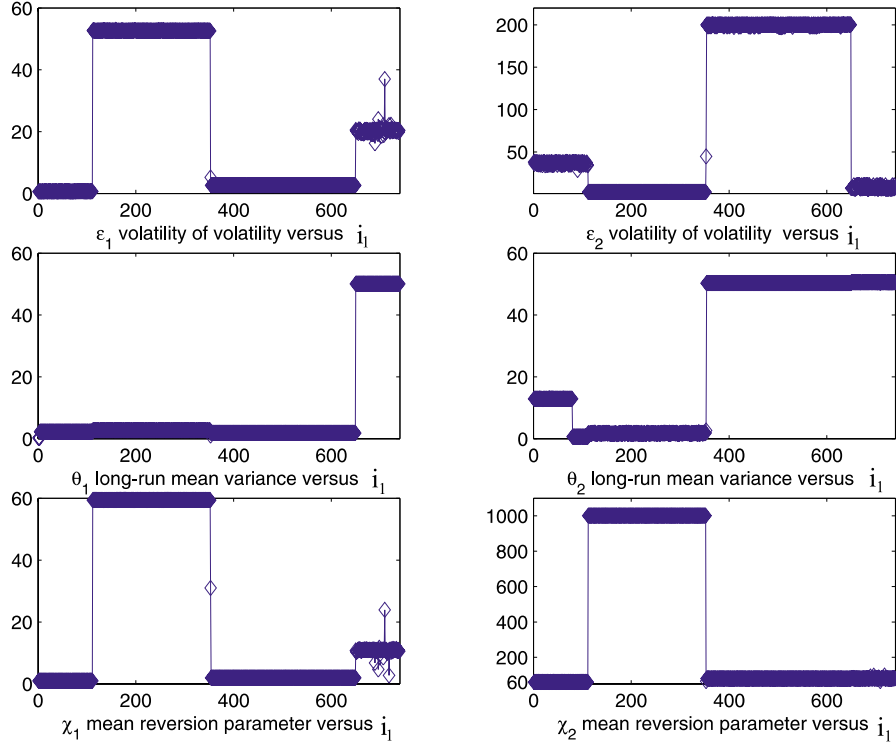


Figure 11: Estimated parameter values obtained solving 740 calibration problems using as data the electric power prices (time series with spikes, Figures 7, 8) versus the calibration problem number i_1 .

calibration procedure produces two values of the ratio χ_1/χ_2 , in particular after the spike (i.e. $i_1 > 100$) there is a jump in the ratio χ_1/χ_2 and we have $\chi_1 \ll \chi_2$.

Figure 11 shows the estimated values of the parameters $\epsilon_i, \theta_i, \chi_i, i = 1, 2$, during the entire observation period covered by the data shown in Figures 7 and 8 (time series with spikes). We note the presence of a big jump in the estimated parameter values around $i_1 = 395$. Note that when we solve the calibration problem corresponding to $i_1 = 395$ we use as data the 26 consecutive daily observations starting with the 395th observation day. That is, this calibration problem takes as input data one of the spikes (see Figure 8) contained in the time series. The fact that Figures 9, 10, 11 show the model parameters as a function of the index i_1 to be approximately piecewise

constant functions suggests that the model and the calibration procedure proposed are well suited to establish a stable relationship between the data and the unknowns of the calibration problem.

Moreover using formulae (4.1), (4.2) and the tracking procedure described in Section 3 we forecast the electric power prices using as data of the calibration problems the data corresponding to the time series containing the spikes (shown in Figures 7, 8). That is we take a data window of 26 consecutive days in the time series of electric power price data we solve the corresponding calibration problem, we use the (approximate) solution of the calibration problem $\underline{\Theta} = \underline{\Theta}^*$ and formulae (4.1), (4.2) to forecast the values of the state variables in the future. The future consists in the time period after the last day whose observation is contained in the data window used in the calibration problem. The data window used as input data of the calibration problem is rolled through the time series using the procedure described previously.

Table 1 establishes the quality of the forecasted values of the electric power log-returns when we do forecasts up to fifteen days in the future and we process the data corresponding to the time series shown in Figures 7, 8. That is Table 1 contains the mean value of the relative error, $e_{log-return}$, committed approximating the observed log-return with the forecasted log-return, the column *trend* contains (in percent) the number of times that the forecasted log-return moves in the correct direction with respect to the log-return of the first day contained in the data used in the calibration, that is increases when the historical log-return increases and decreases when the historical log-return decreases. The last column $e_{log-return, i_1 \leq 100}$ contains the same quantity than $e_{log-return}$ computed on the log-returns observed before the first spike, that is for $i_1 \leq 100$. In Table 1 we consider forecasts 1, 2, 3, 4, 5 and 15 days in the futures, the quantities shown in the Table 1 show how the quality of the forecasts deteriorates when we go deeper in the future.

Finally Figures 12 and 13 show the forecasted values of the log-return (one day in the future) and the time series of the log-returns corresponding to the time series shown in Figures 7, 8 as a function of time t (days). Figure 13 reproduces on a different scale the part of Figure 12 corresponding to $300 \leq t \leq 500$. This is the region where severe spikes occur (see Figures 7, 8). Figures 12 and 13 show the very high quality of the (one day in the future) forecasted log-returns in a more convincing way than Table 1 where we consider highly aggregated performance indices.

<i>number of days in the future</i>	$e_{log-return}$	$trend (\%)$	$e_{log-return, i_1 \leq 100}$
1	0.0485	90.53%	0.0167
2	0.0786	82.27%	0.0268
3	0.0968	77.54%	0.0310
4	0.1078	73.88%	0.0324
5	0.1131	72.94%	0.0322
15	0.1773	63.06%	0.0474

Table 1: Mean relative errors of the forecasted values of the electric power log-returns of the time series with spikes when compared to the log-returns actually observed.

The third numerical experiment consists in the analysis of the daily closing values of the S&P 500 index and of the daily bid prices of the European call and put options on the S&P 500 index with maturity date December 16, 2005 and strike price $K = 1200$ during the period of about eleven months that goes from January 3, 2005 to November 28, 2005. Due to the number of trading days in the year 2005 the time unit is a “year” made of 253 days. Note that the call and the put options mentioned above whose prices have been used as data in this experiment during the period January, November, 2005 have a significant volume traded. To avoid excessive numerical work we analyze in detail the market data (i.e. S&P 500 index and the European vanilla call and put option prices on this index) only in the months of January, February, May, June, October and November, 2005. The results presented are representative of the results obtainable from an exhaustive analysis of the eleven months of data available. We have solved the calibration problem (3.13) using the data contained in a window made of fifteen consecutive observation days, that is fifteen daily observations of the log-return of the S&P 500 index and of the call and put option prices on *S&P* 500 index having maturity time December 16, 2005 and strike price $K = 1200$. In this data window there are three data for each day of observation and fifteen days of observation, that is there are 45 data.

We solve three calibration problems, the first one uses as data the data relative to the first fifteen observation days of January 2005, the second one

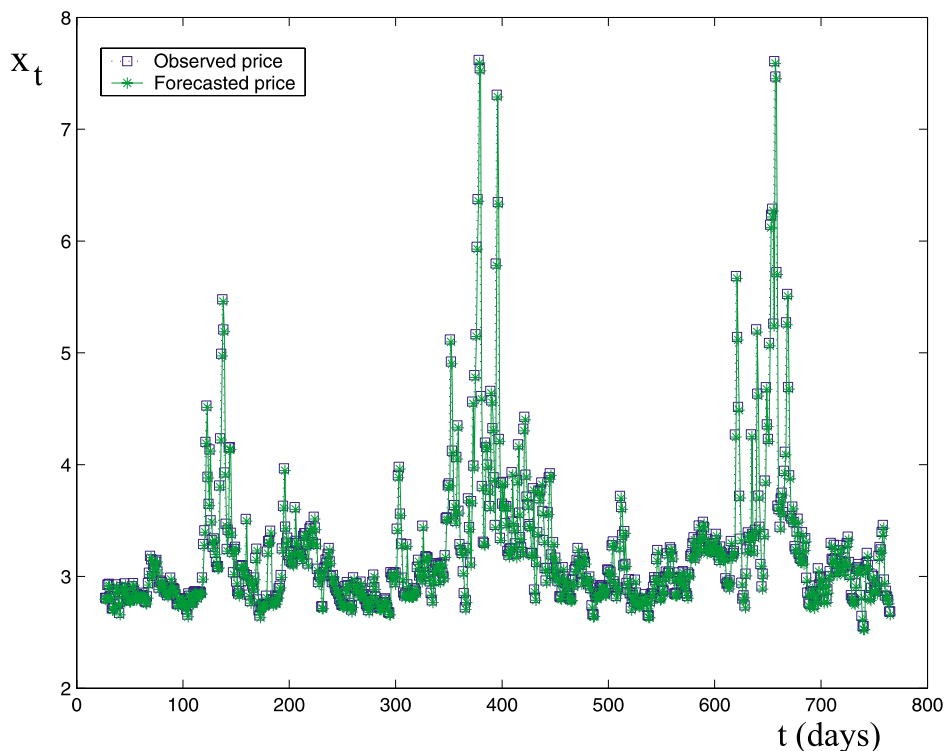


Figure 12: Forecasted values (one day in the future) (stars) and observed values (squares) of the log-returns of electric power prices (time series with spikes, Figures 7, 8) versus time t (days).

uses as data the data relative to the last twelve observation days of May 2005 and the first three observation days of June 2005, and the third one uses as data the data relative to the last twelve observation days of October 2005 and the first three observation days of November 2005. The three sets of estimated parameter values obtained solving these three calibration problems are used to forecast the value of the S&P 500 and the prices of its call and put European vanilla options one day, one week and one month in the future (that is one day, one week, one month after the day of the last observation contained in the data used in the calibration problem). The quality of these forecasts is established by comparison with the corresponding historical data. Moreover a comparison of the results obtained using the calibration procedure proposed here with the results obtained using the least squares formulation of the calibration problem proposed in [11] is presented.

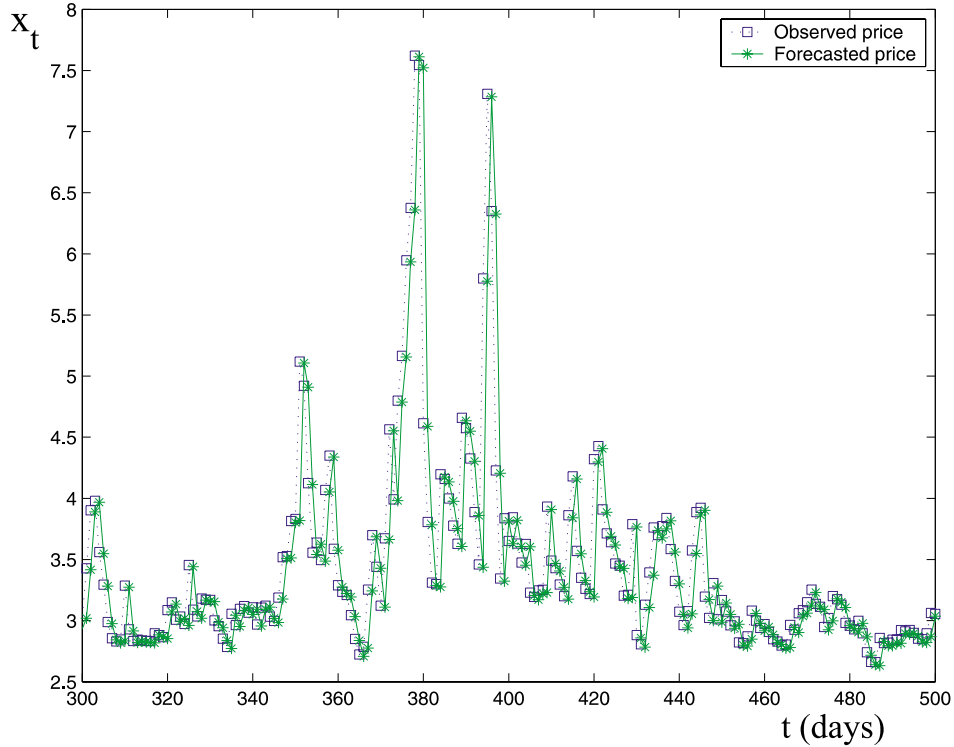


Figure 13: Forecasted values (one day in the future) (stars) and observed values (squares) of the log-returns of electric power prices (time series with spikes, Figures 7, 8) versus time t (days).

The forecast of the S& P 500 index is done with the tracking procedure derived from (4.1), (4.2) already discussed. The forecast of the option prices is done using formulae (2.24), (2.28) starting from the model parameters, including the correlation coefficients, the risk premium parameters and the initial stochastic variances, estimated solving the calibration problem. We use formulae (2.24), (2.28) with two different choices of asset price, that is: the price actually observed in the day of the forecast or the asset price forecasted using formula (4.1). The first choice is considered in order to compare the results obtained in this paper with those presented in [11] where the asset price actually observed the day of the forecast was used. We note that in (2.24), (2.28) we use always the values of the stochastic variances obtained using formula (4.2). That is, given the stochastic variances $v_{1,t}$, $v_{2,t}$, at time $t = t_0 = \tilde{t}_0$ where \tilde{t}_0 is the time of the first observation used

in the calibration problem (that is given the initial stochastic variances $\tilde{v}_{i,0}$, $i = 1, 2$ that are estimated solving the calibration problem) we forecast $v_{1,t}$, $v_{2,t}$, $t > t_0$, using formula (4.2) where the vector $\underline{\Theta}$ is chosen to be the vector $\underline{\Theta}^*$ obtained as solution of the calibration problem. Starting from the solution of the first calibration problem (data corresponding to the first fifteen observation days of January 2005) we forecast the index value and the option prices. In Table 2 we show the relative errors made in the forecast of the *S&P 500* index value e_{index} and of the bid prices of the European vanilla call option, $e_{call\ option}$, and put option, $e_{put\ option}$, having strike price $K = 1200$ and maturity time T given by December 16, 2005 obtained forecasting up to a month in the future. In Table 2 the option prices are forecasted using as asset price the forecasted values of the *S&P 500* index in the days of the forecasts. The errors are computed comparing the forecasted values with the historical data. The results shown in Table 2 relative to January and February, 2005 are somehow representative of the results obtained with a more exhaustive analysis of the data available. Note that the forecasted values of the *S&P 500* index are really satisfactory and of much higher quality than the forecasted values of the electric power prices (compare Table 1 and Table 2). This difference is due to two facts: the first one is the use of the option prices in the calibration procedure when we study the *S&P 500* data. The option prices improve the quality of the solution of the calibration problem and of the conditioned probability densities. No option prices are used in the solution of the calibration problem for the electric power price data. The second one is the huge historical volatility of the time series of the electric power price data. This last fact makes the forecasting problem for the electric power price data very difficult.

Finally we use the estimated model parameter vectors obtained as solution of the calibration problems to forecast the prices of all the European call options on the *S&P 500* index traded in a given day. The days that we consider are January 28, 2005, June 28, 2005 and November 28, 2005. Note that in the year 2005 we had approximately three hundreds European call options on the *S&P 500* index traded. The forecast of the option prices of January 28, 2005 is done using the vector $\underline{\Theta}$ obtained solving the calibration problem using as data the first fifteen observation days of January 2005. The forecast of the option prices of June 28, 2005 and November 28, 2005 are done using as data the first three observation days of the current month (June and November respectively) and the last twelve observation days of the previous month

<i>number of days in the future</i>	e_{index}	$e_{call\ option}$	$e_{put\ option}$
1	$7.522 \cdot 10^{-5}$	0.0659	0.0407
2	$1.303 \cdot 10^{-4}$	0.0559	0.0737
3	$1.7509 \cdot 10^{-4}$	0.0893	0.0952
4	$2.6962 \cdot 10^{-4}$	0.0528	0.0793
5	$2.9114 \cdot 10^{-4}$	0.0496	0.0822
15	$3.7106 \cdot 10^{-4}$	0.0268	0.1810
30	$3.5094 \cdot 10^{-4}$	0.0717	0.1099

Table 2: Relative errors of the forecasted values of the SP&500 and of the corresponding call and put option prices in January and February 2005 when compared to the prices actually observed. The model parameters employed have been obtained solving the calibration problem using as data the data relative to the first fifteen observation days of January 2005.

(May and October respectively). We consider the days January 28, June 28, November 28, 2005 because we have at our disposal the results presented in [11] relative to the forecasts of the call option prices of these three days made using the model parameter vectors obtained as solution of the calibration problem formulated with the least squares procedure discussed in [11]. We compare the call option prices obtained solving the calibration problem with the maximum likelihood procedure presented in this paper with those obtained solving the calibration problem with the least squares procedure introduced in [11]. Let us introduce some notation necessary to illustrate the comparison. Let n_{obs} be the number of call option prices available at time \tilde{t} and let $C^{\tilde{t}}(T_i, K_i, \tilde{S}_{\tilde{t}})$, $C_{LS}^{\tilde{t}, \Theta}(T_i, K_i, \tilde{S}_{\tilde{t}})$, $C_{ML}^{\tilde{t}, \Theta}(T_i, K_i, \tilde{S}_{\tilde{t}})$ denote respectively the (observed) prices at time \tilde{t} of European call options with strike price K_i and maturity time T_i , the prices generated using formula (2.24) with the parameter vector obtained solving the calibration problem with the least squares procedure (LS) and with the parameter vector obtained solving the calibration problem using the maximum likelihood procedure (ML). Note that n_{obs} may depend on \tilde{t} , we omit this dependence for simplicity. Figures

Date t	$\epsilon_{mean,ML}^t$	$\epsilon_{mean,LS}^t$
January 28, 2005	$4.69 \cdot 10^{-3}$	$2.84 \cdot 10^{-3}$
June 7, 2005	$5.99 \cdot 10^{-3}$	$1.75 \cdot 10^{-3}$
June 28, 2005	$6.87 \cdot 10^{-3}$	$2.56 \cdot 10^{-3}$
November 7, 2005	$3.68 \cdot 10^{-3}$	$3.04 \cdot 10^{-3}$
November 14, 2005	$3.07 \cdot 10^{-3}$	$2.21 \cdot 10^{-3}$
November 28, 2005	$3.21 \cdot 10^{-3}$	$2.41 \cdot 10^{-3}$

Table 3: Quality of the forecasted values of the option prices established comparing the forecasted prices with the prices actually observed when the maximum likelihood (ML) or the least squares (LS) method are used in the calibration of the multiscale model.

14, 15, 16 show the absolute error:

$$\epsilon_{C/S_0} = \left| \frac{C_A^{\tilde{t}, \Theta}(T, K, S_0)}{S_0} - \frac{C^{\tilde{t}}(T, K, S_0)}{S_0} \right|, \quad A = LS, ML, \quad (4.3)$$

obtained using the two calibration procedures ($A = LS$ (least squares procedure), ML (maximum likelihood procedure)) as a function of the moneyness $K/S_0 = K_i/S_0$, $i = 1, 2, \dots, n_{obs}$, where $S_0 = \tilde{S}_{\tilde{t}}$ is the value of the S&P 500 index at the transaction day \tilde{t} where the option prices are forecasted and as a function of the time to maturity $\tau_i = T_i - \tilde{t}$, $i = 1, 2, \dots, n_{obs}$. In Table 3 we show the mean error:

$$\epsilon_{mean,A}^t = \frac{1}{n_{obs}} \sum_{i=1}^{n_{obs}} \left| \frac{C_A^{\tilde{t}, \Theta}(T_i, K_i, S_0)}{S_0} - \frac{C^{\tilde{t}}(T_i, K_i, S_0)}{S_0} \right|, \quad A = LS, ML. \quad (4.4)$$

Note that the absolute errors shown in Figures 14, 15, 16 and the mean absolute errors shown in Table 3 are referred to quantities roughly speaking of order 0.1.

We recall that in [11] we have solved three calibration problems using the least squares formulation and the call option price data of January 3, 2005, June 3, 2005 and November 3, 2005. Note that the least squares procedure to solve the calibration problem of January 3, 2005 uses $n_{obs} = 281$ call option prices. Similarly the calibration problem of June 3, 2005 uses $n_{obs} = 281$ call option prices and the calibration problem of November 3, 2005 uses the

prices of $n_{obs} = 303$ call options. We use the parameter estimated using the call option prices of January 3, 2005 ($n_{obs} = 281$) to forecast the option prices of January 28, 2005 ($n_{obs} = 258$) and similarly we use the parameters estimated using the call option prices of June 3, 2005 ($n_{obs} = 281$) to forecast the option prices of June 28, 2005 ($n_{obs} = 278$) and the parameters estimated using the call option prices of November 3, 2005 ($n_{obs} = 303$) to forecast the option prices of November 28, 2005 ($n_{obs} = 292$).

We proceed similarly with the parameter values estimated solving the three calibration problems mentioned above with the maximum likelihood procedure. In fact we use the parameters estimated using the first fifteen daily observations of January 2005 of the S& P 500 index and of the prices of the European call and put with $K = 1200$ and T given by December 16, 2005 to forecast the prices of all the call options traded on January 28, 2005. That is we forecast the prices of January 28, 2005 of $n_{obs} = 258$ call options. Moreover we use the parameters estimated using the last twelve observation days of May 2005 and the first three observation days of June 2005 of the S& P 500 index and of the prices of the European call and put with $K = 1200$ and T given by December 16, 2005 to forecast the prices of all the call options traded on June 28, 2005. That is we forecast the prices of June 28, 2005 of $n_{obs} = 278$ call options. Finally, we use the parameters estimated using the last twelve observation days of October 2005 and the first three observation days of November 2005 of the S& P 500 index and of the price of the European call and put options with $K = 1200$ and T given by December 16, 2005 to forecast the prices of all the call options traded on November 28, 2005. That is we forecast the prices of November 28, 2005 of $n_{obs} = 292$ call options.

Table 3 shows the results obtained. Remind that in the forecasts considered in Table 3 we use as value of the S&P 500 index the actual value of the index the day of the forecast and not its forecasted value. The results presented in Table 3 show that the option prices forecasted with the two methods are approximately of the same quality. We can conclude that the maximum likelihood approach to the calibration problem has two advantages when compared to the least squares approach presented in [11]. The first one is that a relatively small number of data is used to calibrate the model. In fact only one European call and one European put option prices and the corresponding value of the index are considered for each day of data and a time window of fifteen consecutive trading days is used as input data

in the calibration problem. This corresponds to fortyfive data. The least squares procedure uses as data all the call options traded in a given day that is approximately three hundreds data. The second one is the fact that the maximum likelihood approach thank to the tracking procedure discussed previously allows to forecast the value of the asset, that is the value of the S&P 500 index. This is a consequence of the solution of the filtering problem. This makes possible to “forecast” option prices without knowing the value of the S&P 500 index the day of the forecast. Finally we note that going back to Table 2 we can say that the parameter values obtained using the maximum likelihood approach give satisfactory results when used to forecast the option prices up to a month in the future.

We believe that the numerical experiments presented here suggest that the multiscale stochastic volatility model introduced in [11] together with the maximum likelihood procedure to solve the calibration problem and the tracking procedure to solve the forecasting problem presented in this paper are a powerful tool to do the analysis of time series of financial data.

Acknowledgments: It is a pleasure to thank V. Kholodnyi and R. Whaley of Platts Analytics Inc. (Boulder, Colorado, USA) for providing us the electric power price data.

References

- [1] Alizadeh, S., Brandt, M., Dielbold, F.: Range-based estimation of stochastic volatility models, *Journal of Finance*, **57**, (2002), 1047-1091.
- [2] Black, F., Scholes, M.: The pricing of options and corporate liabilities, *Journal of Political Economy*, **81**, (1973), 637–659.
- [3] Capelli, P., Mariani, F., Recchioni, M.C., Spinelli, F., Zirilli, F.: Determining a stable relationship between hedge fund index HFRI-Equity and S&P 500 behaviour, using filtering and maximum likelihood, submitted to *Inverse Problems in Science and Engineering* (2008).
- [4] Chernov, M., Gallant, A.R., Ghysels, E., Tauchen, G.: Alternative models for stock price dynamics, *Journal of Econometrics*, **116**, (2003), 225-257.
- [5] Cont, R., Tankov, P.: *Financial modelling with jump processes*, Chapman & Hall/CRC Financial Mathematics Series, Boca Raton, Florida, U.S.A., (2004).
- [6] Daniel, G., Joseph, N.L., Bree, D.S.: Stochastic volatility and the goodness-of-fit of Heston model, *Quantitative Finance*, **5**, (2005), 199-211.
- [7] Duffie, D.: *Asset pricing theory*, Princeton University Press, Princeton, New Jersey, U.S.A., (2001).
- [8] Fatone, L., Mariani, F., Recchioni, M.C., Zirilli, F.: Maximum likelihood estimation of the parameters of a system of stochastic differential equations that models the returns of the index of some classes of hedge funds, *Journal of Inverse and Ill-Posed Problems*, **15**, (2007), 329-362.
- [9] Fatone, L., Mariani, F., Recchioni, M.C., Zirilli, F.: The calibration of the Heston stochastic volatility model using filtering and maximum likelihood methods, to appear in *Proceedings of Dynamic Systems and Applications*, **5**, (2008).
- [10] Fatone, L., Mariani, F., Recchioni, M.C., Zirilli, F.: Calibration of a multiscale stochastic volatility model using as data European option prices, submitted to *Proceedings MAF08*.

- [11] Fatone, L., Mariani, F., Recchioni, M.C., Zirilli, F.: An explicitly solvable multi-scale stochastic volatility model: option pricing and calibration, to appear in *Journal of Futures Markets*.
- [12] Fiorentini, G., Leon, A., Rubio, G.: Estimation and empirical performance of Heston's stochastic volatility model: the case of thinly traded market, *Journal of Empirical Finance*, **9**, (2002), 225-255.
- [13] Fouque, J.P., Papanicolaou, G., Sircar, R., Solna, K.: Multiscale stochastic volatility asymptotics, *SIAM Journal on Multiscale Modeling and Simulation*, **2**, (2003), 22-42.
- [14] Fouque, J.P., Han, C.H.: Pricing asian options with stochastic volatility, *Quantitative Finance*, **3**, (2003), 353-362.
- [15] Herzel, S., Recchioni, M.C., Zirilli, F.: A quadratically convergent method for linear programming, *Linear Algebra and its Applications*, **152**, (1991), 255-289.
- [16] Heston, S.L.: A closed-form solution for options with stochastic volatility with applications to bond and currency options, *The Review of Financial Studies*, **6**, (1993), 327-343.
- [17] Heston, S.L., Nandi, S.: A closed form GARCH option pricing model, *The Review of Financial Studies*, **13**, (2000), 585-625.
- [18] Jazwinski A.H.: *Stochastic processes and filtering theory*, Academic Press, New York, U.S.A., (1970).
- [19] Lipton, A.: *Mathematical methods for foreign exchange*, World Scientific Publishing Co. Pte. Ltd, Singapore, (2001).
- [20] Mariani, F., Pacelli, G., Zirilli, F.: Maximum likelihood estimation of the Heston stochastic volatility model using asset and option prices: an application of nonlinear filtering theory, *Optimization Letters*, **2**, (2008), 177-222.
- [21] Mordecai, A.: *Nonlinear Programming: Analysis and Methods*, Dover Publishing, New York, U.S.A., (2003).
- [22] Oberhettinger, F.: *Fourier transforms of distributions and their inverses. A collection of tables*, Academic Press, New York, U.S.A., (1973).

- [23] Schoutens, W.: Lévy processes in finance, Wiley & Sons, Chichester, U.K., (2003).
- [24] Silva, A.C., Yakovenko, V.M.: Comparison between the probability distribution of returns in the Heston model and empirical data for stock indexes, *Physica A*, **324**, (2003), 303-310.
- [25] Wong, H.Y., Chan, C.M.: Lookback options and dynamic fund protection under multiscale stochastic volatility, *Insurance Mathematics and Economics*, **40**, (2007), 357-385.

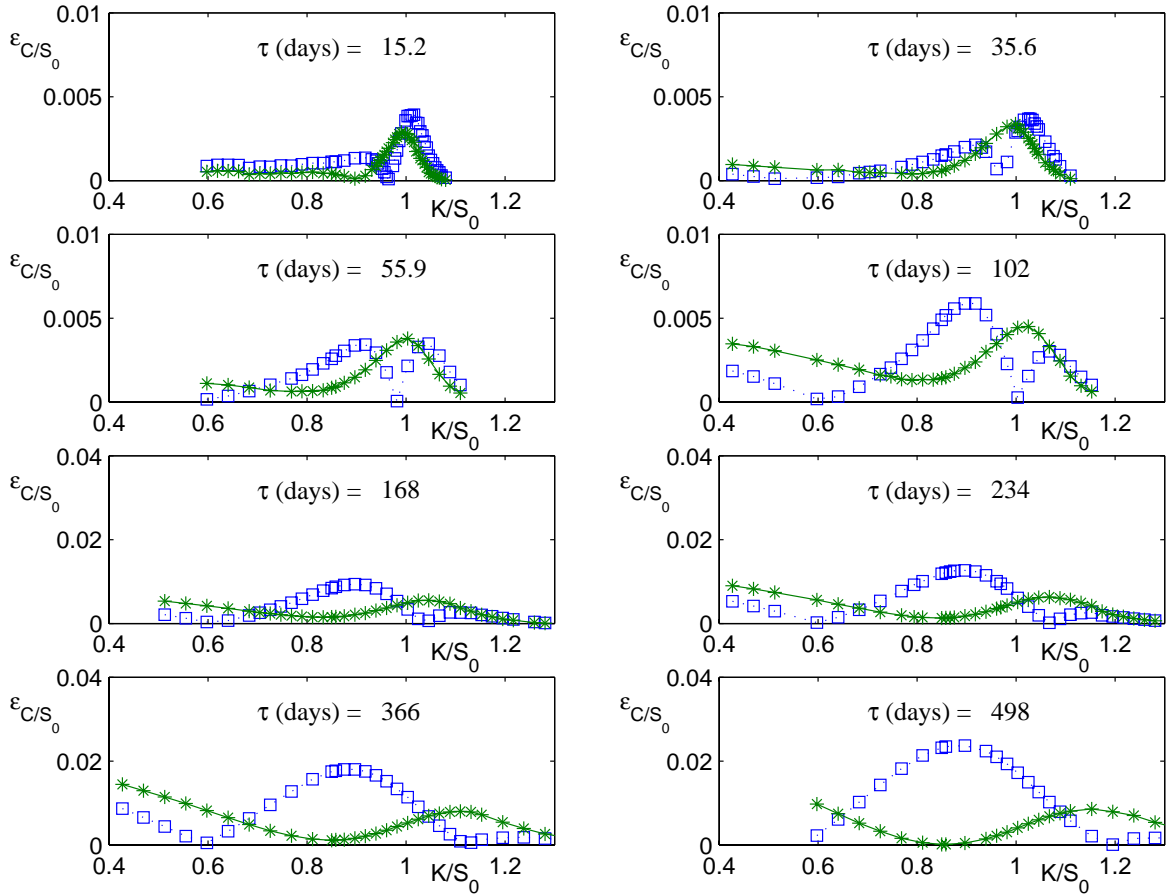


Figure 14: January 28, 2005: Absolute error ϵ_{C/S_0} on the observed call option prices divided by S_0 committed using the forecasted prices obtained using the multiscale model calibrated with the maximum likelihood approach (squares and blue-line) or with the least squares approach (stars and green line) versus moneyness K/S_0 . The forecasted prices are obtained using the same parameter values (resulting from the calibration) for all the maturities considered.

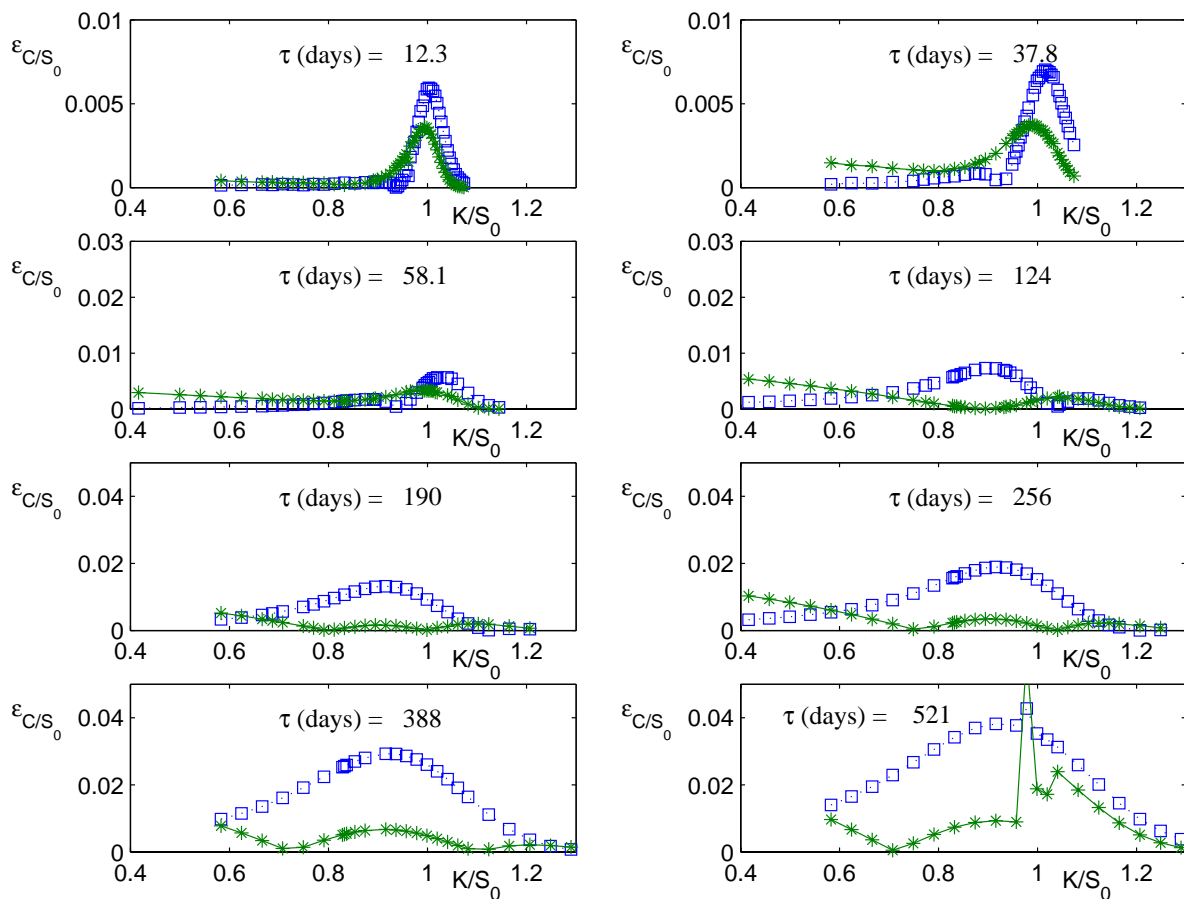


Figure 15: June 28, 2005: Absolute error ϵ_{C/S_0} on the observed call option prices divided by S_0 committed using the forecasted prices obtained using the multiscale model calibrated with the maximum likelihood approach (squares and blue-line) or with the least squares approach (stars and green line) versus moneyness K/S_0 . The forecasted prices are obtained using the same parameter values (resulting from the calibration) for all the maturities considered.

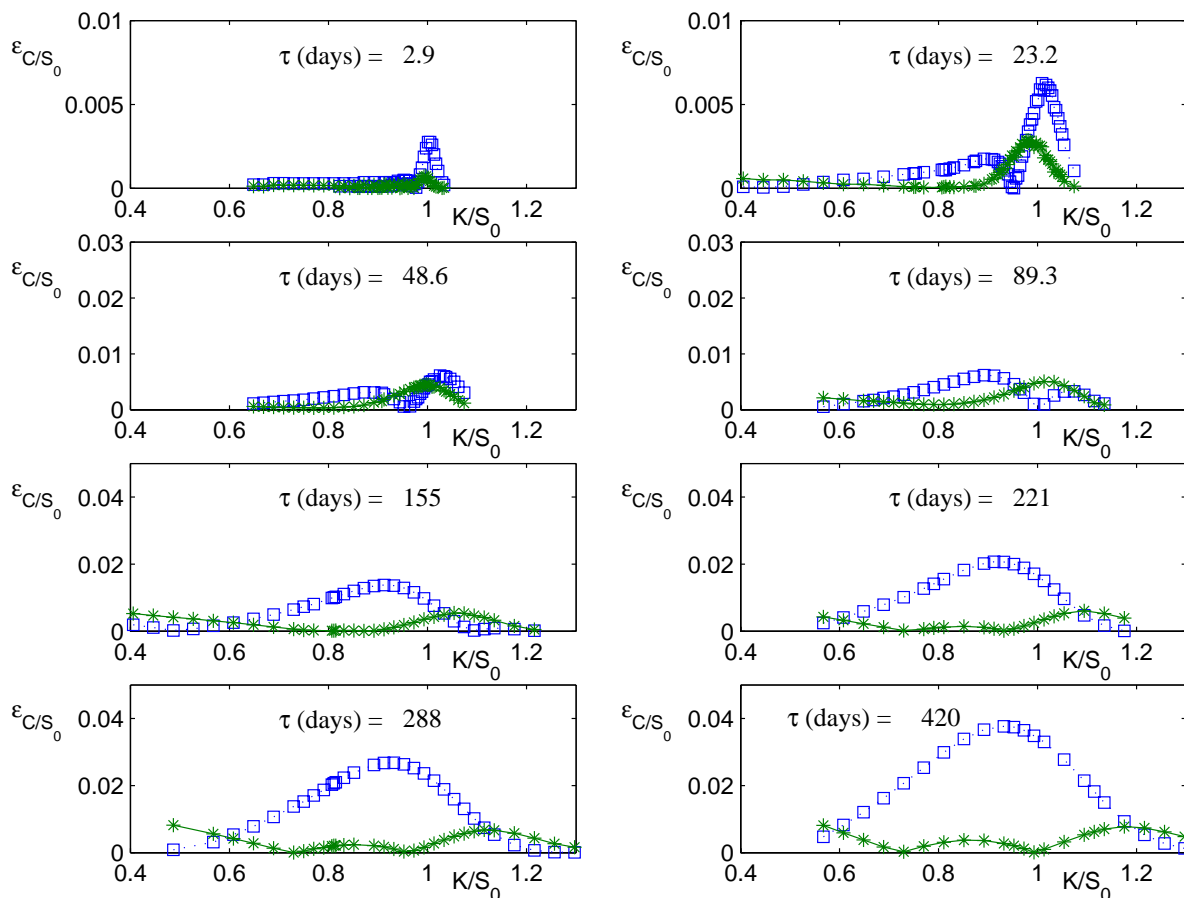


Figure 16: November 28, 2005: Absolute error ϵ_{C/S_0} on the observed call option prices divided by S_0 committed using the forecasted prices obtained using the multiscale model calibrated with the maximum likelihood approach (squares and blue-line) or with the least squares approach (stars and green line) versus moneyness K/S_0 . The forecasted prices are obtained using the same parameter values (resulting from the calibration) for all the maturities considered.